FLASH
Flexible Laser-Based Manufacturing

D1 – FLASH industrial requirements and system specification

HORIZON-CL4-2023-TWIN-TRANSITION-01-02.

Co-funded by the European Union

Funded by the European Union. Views and opinions expressed are however those of the author(s) only and do not necessarily reflect those of the European Union or the European Health and Digital Executive Agency. Neither the European Union nor the granting authority can be held responsible for them.

Co-funded by the European Union

FLASH

Flexible Laser-Based Manufacturing

Revision	Date	Author/Organisation	Description
1st	23 July 2024	MTC	Initial draft
2nd	31 July 2024	All	First review
3rd	01 August 2024	All	Final review
4th			

Grant Agreement Number: 101138380	
Project title: Flexible Laser-Based Manufacturing through Precision Photon Distribution	
Project Acronym: FLASH	**Funding Scheme:** Research and Innovation action
Start Date: 1 January 2024	**End Date:** 31 December 2026
EC Project Officer: Ozlem Cangar	Email: Ozlem.Cangar@ec.europa.eu
Deliverable Number: D1.1	**Deliverable name:** Review of case studies & refined detailed system requirements
Work Package Number: 1 – T1.1, and T1.5	
Date of Delivery: 12/07/2024	
Status:	Draft ☒ Final ☐
Deliverable Type:	Report ☒ Other ☐
Distribution Type:	Public ☐ Consortium ☒
Authoring Partner: MTC	
Contact Person: Dr. Mitchell Leering	
Email: Mitchell.Leering@the-mtc.org	**Phone:** +44 7566 775995
Keywords:	Flash Project, Laser, Manufacturing, End-Users, System Specification
Name of the representative of the Project Co-ordinator, Title and Organisation	**Name:** Dr Gaetano Patrimia **Organisation:** Prima Additive **Tel:** +39 011 410 36 24 **E-mail:** gaetano.patrimia@primaadditive.com

Executive Summary

The FLASH project aims to shift the perspective of conventional manufacturing by exploiting a flexible and customisable laser-based production system. This project combines multiple lasers and beam delivery approaches with advanced fully three-dimensional dynamic beam shaping, housed in a single machine platform to achieve highly customised laser cutting, drilling, surfacing and welding. The project end-users will provide use-cases to demonstrate the full capabilities of the developed system for its use in medical, automotive, automation and advanced tooling applications.

This deliverable has aimed to capture the activities and outputs achieved in Tasks 1.1 – Review case studies and refine detailed system requirements and 1.5 – Refine specifications for the system from Work Package 1 of the Flash project.

The initial part of this deliverable provides a detailed review of each end-user case study. It outlines the analysis of the currently deployed manufacturing processes. It defines the requirements for the demonstration of the Flash system in terms of the components, materials, laser-based manufacturing processes, analysis and functional evaluation per use case. Emphasis has been placed on gathering business and operational requirements of the intended Flash components to identify key KPIs for each manufacturing use-case, ensuring the alignment of the Flash machine platform specification/capability to the intended process targets. Performance against operational targets will be routinely scrutinised throughout the remaining work packages and may require further modification/elaboration based on the outputs of the Flash project. Additionally, information on component lifecycle, environmental and conventional processes was collected, providing the initial basis for formulating the Life Cycle Analysis.

The remainder of the deliverable describes the first iteration of the specification of the Flash machine system. This machine platform will integrate three distinct laser sources (high power near-infrared and two ns green lasers) which will combine with three possible beam delivery methods, notably, nozzle-based, galvoscanner, or WJGL delivery. The processing performance will be further enhanced by implementing three-dimensional dynamic laser beam shaping (X-Y spatial beam energy and Z-positional focus shifting) capabilities. Two dedicated in-line monitoring (optical and acoustic) systems will ensure the consistency and quality of the production system. A closed-loop control software, driven by machine learning, will act on any detected process deviations by rapidly modifying processing parameters to ensure optimum success of the outputs. The various associated components within the Flash platform will be developed by respective project partners in work packages 2 to 7.

This task was led by the MTC with the help of all partners within the consortium.

Table of Contents

List of abbreviations

Abbreviation	Full description
FLASH	Flexible Laser-based Manufacturing Through Precision Photon Distribution
ATOP	ATOP S.p.A – IMA Automation
EV	Electric Vehicles
TOFAS	Turk Otomobil Fabrikasi Anonim Sirketi
DPS	Depuy Synthes
DIA	Diamoutils SAS
WJGL	Water Jet Guided Laser
AI	Artificial Intelligence
CCB	Cross Car Beam
PCD	Polycrystalline Diamond
CBN	Carbon Boron Nitride
IMA	Industria Macchine Automatiche SPA
PAI	Polyamide-imides
PEEK	Polyether ether ketone
NIR	Near-infrared
IR	Infrared
IC	Integrated Circuit
CVD	Chemical Vapour Deposition
WC	Tungsten Carbide
GMAW	Gas Metal Arc Weld (Otherwise known as MIG/MAG welding)
LCA	Life Cycle Analysis
QCW	Quasi-Continuous Wave
DPSS	Diode-Pumped Solid-State
WP	Work Package
FCM	Fiber Coupling Module
MPLC	Multi-Plane Light Conversion
IMCs	Intermetallics

1 Introduction

The Flexible Laser-based Manufacturing Through Precision Photon Distribution (FLASH) project aims to develop and demonstrate a flexible and customisable production solution that is enabled by various laser-based manufacturing processes. Traditional manufacturing processes are no longer versatile enough to react to ever-shortening product lifecycles, rapid movements in innovation, and mass customisation required to meet global supply chain demands. Laser-based manufacturing processes are more suited to rapid process changes, require fewer consumables, and generate considerably less waste (e.g. coolant, chips, tools, etc.) than traditional mechanical or chemical techniques. Critically, laser-based processes are well suited to precise digital control and parameterisation. Laser-based manufacturing techniques like cutting, drilling, milling, welding, and surfacing are well-established processes that are generally carried out on individually developed systems. Although these existing laser production technologies are mature, they lack the agility to meet the demands of 'rapid' product development as dedicated laser systems are typically established per production technique. This methodology requires significant initial and re-investment in large capital expenditure to continually expand an equipment offering.

The FLASH project will focus on developing a highly customised laser-based production system that offers multiple laser sources (lower energy short pulse to high power continuous) that can be delivered to the target via a range of beam delivery techniques (nozzle, galvo-scanner, and Water Jet Guided Laser (WJGL) based) in a single machine platform. Parts will be able to be held in the standard CNC fixture of the IANUS cell capable of multi-axis movement and rotation. Innovations in dynamic beam shaping and in-process monitoring will be combined with advanced process simulations and Artificial intelligence (AI) to maximise manufacturing efficiency and reducing the need for expansive experimental laser-process optimisation. This unique combination of systems will be integrated into a single-machine platform, providing vast laser-based manufacturing capabilities.

The benefits of the developed system will be demonstrated in four uniquely different industrial application case studies. These end users are in three critical industries, automation/automotive (ATOP and TOFAS), medical (DePuy Synthes), and high-value tooling (Diamoutils). This report summarizes each end-user case study requirement in terms of business, operational, and experimental development, along with a short review of relevant literature for each use case.

In addition, this document outlines the core system/component specifications of the FLASH system and their respective role and functions within the overall platform. This document is linked to Task 1.1 – Review case studies and Task 1.5 – Refine specifications for the system.

Critical assessment and understanding of the technical specifications of the FLASH systems and end-user requirements are crucial for the successful implementation and demonstration of the developed machine platform and the wider project. The FLASH project consortium intends to develop the system to the highest possible technical standards to ensure the system meets all safety standards and satisfies the requirements set out in the end-user case studies.

2 Review of industrial end-use cases

This section provides a detailed analysis of the four individual end-use cases and their respective components that will be used to demonstrate and evaluate the effectiveness of the FLASH system. The application and general industry of the four FLASH end-use cases are summarised in Table 2-1. FLASH brings together several key partners, technologies, and knowledge bases that will empower a significant shift across many strategic manufacturing industries such as medical, tooling, automotive, and e-mobility. FLASH will explore five industrial case studies across four industry sectors.

Table 2-1. Summary of end-use cases

Company	Application	Industry	Location
ATOP S.p.A (ATOP)	Laser stripping and welding of copper hairpin wires for Electric Vehicle (EV) motors	Automation & automotive	Italy
Turk Otomobil Fabrikasi Anonim Sirketi (TOFAS)	Laser cutting and welding of multi-metallic material Car Cross Beams (CCB)	Automotive	Turkey
Depuy Synthes (DPS)	Laser machining of the acetabular cup from orthopaedic hip implants	Medical	Ireland
Diamoutils SAS (DIA)	Laser machining and surfacing of Polycrystalline Diamond (PCD) drill bits & super abrasive grinding wheels	Advanced tooling	France

A short review of the relevant literature on each end-use case has been provided in

Appendix A.

2.1 ATOP – Stripping and welding of copper hairpin wires for electric motors

ATOP is a subsidiary company of the Industria Macchine Automatiche SPA (IMA) group. The manufacture of machines and automatic lines for electric motor production is a core element of their business. ATOP is a world leader in the field of electric drives for sustainable mobility, household appliances, and power tools [1].

2.1.1 Current process and challenge

Copper hairpin windings configurations are the industry standard for windings in traction applications for electric vehicles. Unlike the traditional thin wire coil winding schemes, the hairpins are produced from solid, enamelled copper wires, as shown in Figure 2-1.a. The polymeric insulation layer is typically Polyamide-imides (PAI) or Polyether ether ketone (PEEK). The wires' circular or rectangular cross-sectional dimensions vary by case but largely range in size from 2-6 mm. The benefit of thicker solid sections allows for higher current flow by maximising functional material volume in each area. The production steps to form the winding scheme around a motor stator stack consist of: first, removal of the insulating coating at the joint area, secondly, shaping, thirdly, directly inserting each hairpin, and aligning the ends to be joined, finally the hairpin ends are electrically contacted, typically by laser welding, to form a continuous winding scheme [2]. These process steps are demonstrated schematically in Figure 2-1.b [3].

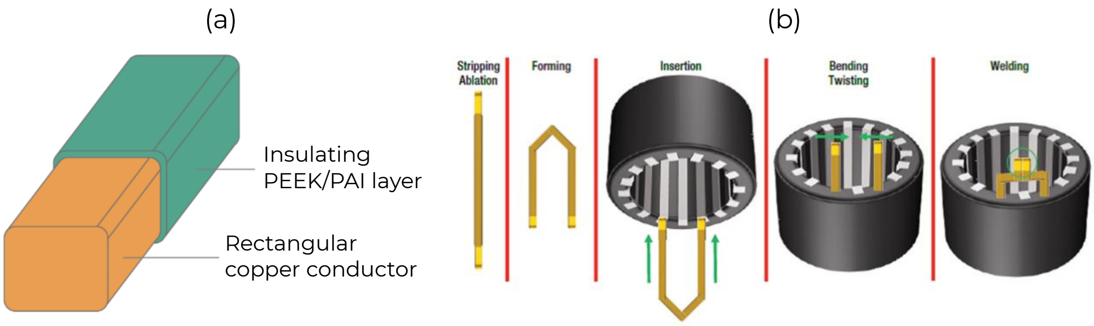

Figure 2-1. (a) Example of enamelled copper hairpin wire, (b) hairpin assembly stages [3]

Before welding, the insulating material must be removed at the joint area to ensure an optimal connection. It is critical to achieve residue-free removal to prevent the entrapment of the isolating material as this can lead to the formation of porosity in the joint, drastically lowering the structural integrity of the joint. Due to the large number of contacts prepared during the manufacture of traction motors, it is essential to use a productive and repeatable wire stripping process that results in a residue-free surface, whilst not removing or affecting the underlying copper material. The most widely used removal process is mechanical milling, using multiple tools with diamond inserts or melting by induction. Removal by lasers offers a contact- and residue-free process with minimal process hindrances. To date, several laser-based methods, such as bulk stripping using a CO_2 laser followed by a secondary cleaning pass with an ns fibre laser. Although this has been investigated for hairpin stripping, this method is not widely industrialised due to the high associated CAPEX cost, complexity, and lower productivity of CO_2 lasers [4].

Once successfully stripped, the wires are joined, typically by laser welding, forming a winding network. Although limited in number, several publications outline the use of various laser types for welding copper hairpin joints, these are outlined in

Appendix A. However, copper has an absorption coefficient of as low as 5% for lasers that operate in the infrared (IR) range. High-power density lasers, operating with a few kilowatts of average power, are used to overcome this lack of absorption. This can result in unwanted effects such as thermal damage of the remaining desired insulating material and instability of the melt pool, exacerbating the formation of porosity.

ATOP's current stripping processes involve either mechanical (milling) or thermal (near-infrared (NIR) fibre lasers or CO_2 lasers) machining of the PAI or PEEK material. However, these processes are hindered in some cases by significant tool wear, ineffective/incomplete stripping, burned borders of remaining insulation, and dirt and debris accumulation in the equipment. Once they successfully remove the insulating material, a NIR continuous laser is used to weld the hairpins. High variability in the produced welds can occur with the current joining process due to the low energy absorption of copper. Additionally, welding defects such as large amounts of spatter, porosity, and misalignment, all negatively affect the quality and functionality of the overall produced components.

2.1.2 Business and operational requirements

An improved solution for preparing and joining copper hairpins is required to manufacture high-performance electric vehicle motors, that will be required to satisfy the increase in demand and range of electric vehicles. For ATOP to improve its economic viability in this area, it should look to fully remove mechanical tooling operations from its hairpin wire stripping processes, this will eliminate the problem of high tool wear. This can be achieved by fully adopting a flexible laser-based approach that is optimised and benefits from both in-process monitoring and AI for improved control over ATOP's machining and joining processes. Additionally, the ability to carry out both the machining and welding operations on a single machine platform will drastically reduce the overall CAPEX burden, along with streamlining its production capability.

Mechanical wire stripping methods are reported to frequently remove the copper conducting material during the skinning process. Worn tools can also lead to variability in the length of the removed insulating material [4]. Mechanical wire stripping processes are comparable in removal rates (approximately 3 cm^2/cm) to the current state of the art of CO_2 lasers. These very long wavelength laser sources provide a non-contact alternative, illuminating the risk of tool wear and process variability. These factors have led to CO_2 lasers widely used in industrial wire stripping applications. However, the adoption of fibre laser sources for this use case offers advantages such as better processing precision and beam quality through a smaller beam spot size, higher energy efficiency resulting in lower operational costs, significantly more flexibility as processing parameters can be easily altered with fibre laser sources. The higher beam quality of fibre lasers is expected to result in an estimated 300% increase in productivity to ~12 cm^2/s compared to conventional CO_2 and mechanical methods, this is as a result of switching to a fibre laser source.

Regarding the welding of the hairpins, incorporating the dual laser sources (1080 nm and 515 nm) provided in the FLASH system will increase the laser absorption from 5% to up to 40% (copper has a significantly higher absorption coefficient at shorter wavelengths). This will enable more efficient welding at lower average powers with an associated reduction in overall process energy consumption. For example, a ~35% reduction in input energy was observed by Kellens et al. when halving the output power in laser cutting operations with a comparable fibre laser system [5]. The improved penetration of the absorbed laser energy will drastically increase the weld process efficiency and quality leading to a reduction in the formation of porosity. This will lead to increased joint strength, higher motor performance (lower electrical resistivity), and longer service life of the produced motors. Consumable costs and machine downtime associated with the frequent replacement of damaged safety screens due to spatter can be reduced through improved control of the weld pool dynamics with the beam shaping and lower average welding power.

Most critically, the reduction in the overall current process rejects rates (0.5% of total stripping and 1.5% of total welding operations on a 200,000 e-motors production line) is imperative as each wasted stator assembly represents a loss of over €1000. The adoption of the FLASH laser-based production system is expected to reduce scrappage by up to 25% and energy consumption by 60% through the combination of the dual-wavelength laser set-up, online monitoring system, and a Life Cycle Analysis (LCA) guided process design tools. The FLASH system will overcome significant commercial challenges for laser adoption by enabling laser stripping and welding on a single platform, this will reduce required investment costs and save over €950,000 annually.

2.1.3 Approach

ATOP's case study will investigate both laser machining and welding to fulfil multiple functions: increase material removal rates of the insulating layer without damaging underlying conducting wire, remove any remaining residue left after stripping, and achieve fast welding rates while reducing porosity formation. It is anticipated that two laser sources (1080 nm NIR CW/ms and 515 nm green short ns), two beam delivery methods (nozzle- and galvoscanner-based), in-process monitoring, beam-shaping, and AI-driven process optimisation (based on experimental and simulation results) will be required to achieve these specified targets. Figure 2-2 provides a schematic representation of the skinning and welding process for hairpin welding.

The representative material that will be used to demonstrate this end-use case will be copper wires, coated in insulating PAI or PEEK, with a rectangular section ranging from 2x2 mm to 6x4 mm. A minimum hairpin length of 30 mm is to be stripped on all four sides. The ends of the hairpins will be welded without the need for filler material. Four individual process steps will be deployed in this demonstration.

1. Cutting of the raw material to the required size using a CW/ms laser and nozzle-based beam delivery.
2. Bulk removal of the insulating material on all sides of the hairpin using a CW/ms laser with a galvoscanner-based beam delivery.
3. Surface cleaning of the exposed copper areas to remove remaining residue and dirt before joining, using the short pulse ns 50 W green laser (515 nm) with a galvoscanner beam delivery.
4. Joining of clamped adjacent copper ends by the hybrid dual beam (1080 nm + 515 nm) and galvo-based laser welding.

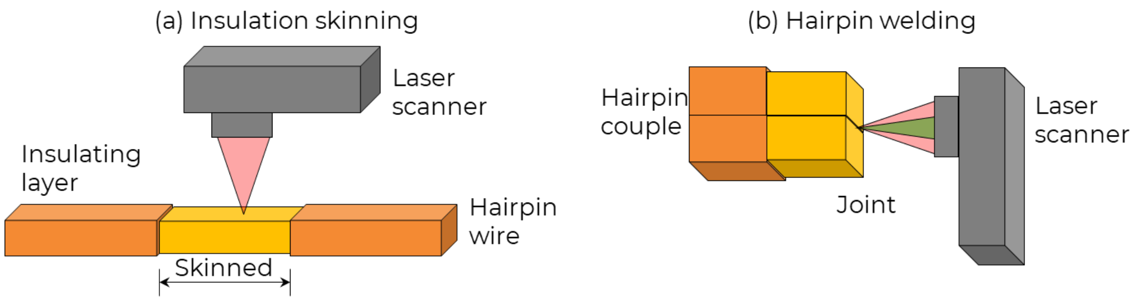

Figure 2-2. Schematic representation of (a) wire stripping and (b) hairpin welding

The CW/ms laser (1080 nm) is highly suited for the bulk removal of the insulating layer as it will be rapidly heated and removed through a combination of ablation, melting, and ejection. The poor absorption of NIR laser energy by copper will leave the conducting material largely unaffected, except for some localised heating. The short pulse ns laser will follow to ensure the ablation of the remaining insulating residue and dirt on the exposed copper surface.

Copper is notoriously difficult to weld with lasers at longer (>600 nm) wavelengths. Conventionally, higher average processing powers are used to overcome the lack of absorption of the laser energy. This creates surface damage such as burrs which require further processing. Additionally, copper has high thermal conductivity, leading to rapid heat dissipation and difficulty maintaining a stable weld pool. The FLASH dual-laser platform will enable both the CW/ms and green ns laser to be used in a coaxial beam delivery to overcome these challenges. The short ns green (515 nm) laser will be pulsed at a sufficiently high-power density to establish the melt/keyhole at the joint location. The CW/ms laser will operate simultaneously with larger average powers to maintain the melt pool stability and increase the penetration depth of the weld. This approach will increase the productivity and quality compared to conventional IR laser-based welding of copper.

2.1.4 Evaluation methodology

Evaluation of the product produced by the FLASH system will be benchmarked against existing production methods by ATOP. To date, there are no direct standards and legislation for the assessment of hairpin stripping and welding. However, all produced hairpins will be assessed according to ATOP's internal criteria and procedures, which are broadly outlined below:

Wire stripping:

- Ability of developed processes to meet minimum productivity, reliability, and cost targets compared to conventional mechanical/thermal processes.
- Control of the residual stripping material to achieve a measured carbon percentage of ~0% without the removal of any conducting material.
- Relative Fluorescent Unit measurements and optical microscopy will be used to assess the overall removal of the insulating layer.

Hairpin welding:

- Ability to complete the welding process in the defined minimum processing time of less than 200 ms whilst meeting stringent weld quality and strength requirements.
- Hairpin tensile tests to be conducted to full fracture, to determine maximum load. Followed by optical microscopy to identify the volume of welding pores.

In addition, acoustic signatures recorded in-process will be evaluated to establish a criterion of ideal machining and welding conditions relative to the processing parameters.

2.1.5 Case study summary

Table 2-2 lists a key summary of the ATOP end-use case.

Table 2-2. Summary of ATOP end-use case

Case study	Preparation and joining of copper hairpins (copper wires with a rectangular cross-section).

Challenges	Laser machining of insulating protective coating and welding copper hairpins.
Objectives/ KPIs	Hairpin stripping: • Bulk removal of PEEK or PAI layer at a material removal rate of 12 cm^2/s to achieve a 70% productivity improvement. Hairpin joining: • Maximum welding time of 200 ms. Overall: • Minimum electrical energy reduction of 60% compared to conventional processes. • Minimum reduction of comparable scrappage rates by 25%. Supporting elements • Online monitoring system and supporting LCA process design tool.
Component	A pack of insulated copper hairpins welded together in a winding scheme to create key components of high-performance EV motors encased in a laminated sheet metal package.
Illustrations	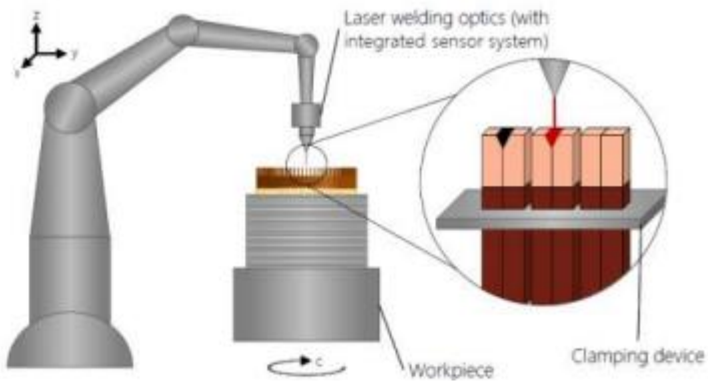 Schematic of the current laser welding of hairpins
Current manufacturing process	Hairpin stripping • Mechanical milling to achieve a residue-free surface using multiple tools with diamond inserts. Hairpin joining • High power density (2-6 kW) IR (1030-1080 nm) CO_2/fibre laser welding of the exposed ends to create an electrical connection.
Currently used materials	Copper hairpins coated with PAI/PEEK. Hairpins of diameter 2-6 mm and a cross-sectional area below 20 mm^2. No information on the thickness of the insulating coating has been provided.
CO_2 impact	To be determined during the remainder of the project.
Current energy demands (kg/yr)	To be determined during the remainder of the project.
Component production /annum	200,000 EV motors per production line per annum.
Functionality	The hairpin welds form a key part of the windings for EV motors and the integrity of the weld directly influences the performance and lifecycle of the motor.
FLASH impact on existing	Increase in the processing rate of laser stripping of protective coatings from copper hairpins. Increasing to 12 cm^2/s from 3 cm^2/s and representing an improvement from a maximum of

manufacturing and savings	7 cm^2/s using current SOTA laser processing. The process will aim for residue-free output. Improvement of the welding process by enabling the efficient creation of a stable, deep penetrating weld pool using less energy. This will lead to a reduction in defects from excessive energy input and resulting higher-quality EV motors.
Processes/Materials to be used with FLASH solution	Materials • PEEK/PAI coated rectangular (2-6 mm diameter) copper wire that is formed into hairpins for motor windings. Process • Laser stripping of protective coating using a microsecond pulse (10-20 µs) 0.5 – 1 kW average power NIR (1080 nm) CW laser. • Laser cleaning of stripped hairpin using 50 W average power nanosecond (5-10 ns) pulsed green (515 nm) laser. • Laser welding of copper ends using hybrid dual beam CW/ms <2kW average power and a >10 kW peak power 10 ns pulsed green laser.

2.2 TOFAS - Welding of metallic cross-car beam

Turk Otomobil Fabrikasi Anonim Sirketi is a global automotive manufacturer, that produces both passenger cars and light commercial vehicles. TOFAS is one of the largest companies in Turkey, with an annual vehicle production rate of over 450,000 vehicles [6].

2.2.1 Current process and challenge

The current product for TOFAS is an assembly consisting of a Cross Car Beam (CCB), a major structural member of a vehicle, additional brackets and functional projections that attach the CCB to the various parts of the surrounding vehicle structure. A CCB serves to provide structural reinforcement and support, enhancing rigidity and safety by distributing forces and minimizing chassis flex during vehicle operation. Currently, various grades of steel are used for the various components in the assembly. The conventional process for producing this crucial component starts with the cutting of steel workpieces from wide-diameter stock. The brackets are stamped from sheet stock and tubes are roll-formed. All projections are cut from stock or formed as appropriate to their required geometries. The pieces are then held in a jig and Gas Metal Arc Welded (GMAW) by robotic manipulation. This fixes the brackets and joins the major structural components. Finally, the projections and fixtures are added using manual welding techniques.

The challenge presented by this is to change the material used for part of the major structural tubular member from steel to aluminium. This alteration will enable lightweighting and will involve dissimilar material welding of steel to aluminium. As the brackets and projections are still to be made of steel, this will necessitate dissimilar welding of a variety of grades and thickness of steel and aluminum. The challenge here is that arc welding of dissimilar materials leads to a low-quality weld due to the formation of intermetallic compounds which embrittle the weld and decrease the strength [7].

One severe issue with steel to aluminium joining, both in welding and also in other more mechanical joints, is if there is any contact between the two metals there is a galvanic difference leading to corrosion. This is particularly a concern in automobile manufacture when there is the concerns of rain and salt spray from gritted roads would accelerate any such corrosion. The galvanic corrosion rate of the two materials is quite high [8] [9] [10]. Typically, in automotive, there are 2 approaches to trying to deal with galvanic corrosion, an intermediate insulating layer or a heavy coating to prevent water ingress. An insulating layer is not necessarily compatible with a welded joint which is why there is a common use of mechanical fixings which permit this. A heavy coating must be certain to be of a high integrity and even then may have certain issues as many cars have had issues with this form of corrosion, particularly those of Land Rover with the Evoque and Discovery steering column [11], Range Rover tailgate and a variety of Stellantis vehicles with panels and hinges [12] among many other easily findable examples.

Laser welding has been explored in the context of achieving dissimilar welding, however, there are significant issues with macro-scale welding, namely the formation of a very brittle intermetallic phase between the materials as well as significant cracking and weld inclusions [13] [14] [15]. There are significant concerns linked to that and the ability to replicate a full steel cross beam in terms of the overall structural robustness of a CCB in an aluminium suitable for welding.

The challenges associated with this project will be whether laser welding is able to overcome the two main issues with dissimilar welding when it comes to the final process and whether an aluminium alloy of sufficient strength will be able to be found so that weight savings can be realised.

2.2.2 Business and operational requirements

TOFAS aims to achieve three main goals with the FLASH system. These are all largely related to productivity and weight enhancements in the current design.

The first aim is an increase in flexibility of design, developing a dissimilar welding process will enable TOFAS to substitute lighter materials for steel where appropriate on the CCB. This is justified in that, substituting steel for aluminium in the structural members will permit a saving of approximately 1.5kg of weight per CCB. This equates to a potential range extension of up to 0.2km in an EV and an accompanying CO_2 saving of 45g/100km. When applied across TOFAS production volume of up to 300’000 cars it will become a significant environmental saving. This will also deliver a process energy saving of 65% achieved through a combination of energy efficiency and a reduction in overall operation time.

The second aim is that of operational costs and timings, the current operation time for this is 900 seconds per CCB, with a weld length of 3654 mm that has an overall operation rate of ~ 4mm/s using conventional welding. The requirement is to increase that to 15 mm/s which will result in a shorter processing time of ~ 240 seconds per CCB. This reduction is expected to deliver up to a 50% operational cost saving through the decrease in process energy requirements and the decrease in operation time.

The third aim is to achieve an improvement in the weld quality, this does not have a quantifiable metric associated with it because it involves a change in materials which comes with an accompanying change in the type of defects which might be expected.

2.2.3 Approach

The planned approach to demonstrate the Flash system with this use case is based on three distinct laser-based processing stages.

The first stage is laser cleaning of the materials to prepare them for welding. This is particularly important for the welding of aluminium because of the surface oxide film. If it is uncleaned this can lead to gas inclusions in the weld as well as contamination owing to the tendency of the oxide to absorb contaminants [16]. Cleaning also improves the surface quality and reduces the tendency for hydrogen porosity to form [17]. These problems with aluminium specifically are in addition to the usual need to prepare a surface for welding to remove contaminants. Laser cleaning has been shown to significantly increase the strength of welds when dealing with dissimilar joints. Wei et. al. [18] showed cleaning led to an increase in material interlocking and consequently higher mechanical strength between 6061 aluminium and 310S Stainless steel.

The next step is that of welding the dissimilar materials (Steel/Aluminium) of sheet/tube wall thicknesses between 0.8 and 4 mm. This will be done using a hybrid welding system using 1080 nm CW and 515 nm ns lasers, or some parameter combination thereof. This is the area that will require the greatest investigation because the technical problem is not a trivial one. Dual-beam welding has shown some promise in the joining of dissimilar materials in copper [19] which has similar issues to steel/aluminium in the formation of brittle intermetallics (IMCs) in welds. Welding of aluminium and steel in general has focused on the use of filler metals either in the form of a brazing filler [20] or the use of an interlining film of a material like nickel [14]. The precise nature of this process may need to be the subject of further specification and investigation to try and find an approach that will work for this process.

The final step will be in cleanup post-welding operation, welding produces several aftereffects on the part including oxides and spatter. In any joining process between aluminium and steel, protective layers should be applied as soon as possible after the process to inhibit galvanic corrosion. Before painting or coating the aluminium, it is necessary to clean the oxide layer as well as any welding by-products. This will employ the short pulse length (ns) green lasers as a cleaning tool, promising results have been shown with a short ns pulse length IR laser by Seo et. al. [21]. Using ns pulse lengths to remove oxide films has been widely studied by many others as a practical process [22]. This will likely be possible to replicate with a green-wavelength laser owing to the increase in absorptivity of that wavelength compared to the IR lasers in the studies.

2.2.4 Evaluation methodology

There will be three key criteria on which this use case will be evaluated.

The first is that of initial weld integrity, is it possible to weld an aluminium alloy of sufficient strength to structural steel and have those welds meet the same performance as the current joints? This will be evaluated by tensile testing as well as microstructural evaluation of the weld to characterise it, observe cracking, formation of IMCs or any porosity as well as the surface quality left afterwards. The precise alloy of aluminium will provide information for a revised design to see whether the thickening of structural parts is necessary to meet automotive design requirements and whether that will reduce potential weight savings. This will provide indicative results as to whether this application is possible with the FLASH system and might be able to deliver TOFAS desired results.

The second criterion is that of weld service life, where there are two areas of most concern with this. The first is that of galvanic corrosion. Representative ageing tests such as a salt spray environment test will be conducted to see what degree of degradation the weld undergoes and what effect that might have on the welded part's durability over its service life. The criteria here will be the degree of lost mechanical properties and the scale of defects such as stress corrosion cracking or aluminium undergoing sacrificial anode oxidation, this will be explored by cross-sections and metallurgical examination of the welds.

The third is process speed, during the development of the welding process, a welding speed will be ideally determined to derive results to an acceptable quality and speed of welding. This will be a simple point of comparison between the current state of 4 mm/s and whatever rate is achieved which produces a weld of satisfactory quality.

2.2.5 Case study summary

Table 2-3 lists a key summary of the TOFAS end-use case.

Table 2-3. Summary of TOFAS end-use case

Case study	Welding of aluminium CCB components to steel retainers and components.
Challenges	Development of a multi-step process to prepare, shape and weld CCB to replace existing discrete processes. Adaption of laser-based processes to enable lighter alloys where possible and to overcome processing challenges of dissimilar welding, processing time and thermal distortion.
Objectives/ KPIs	Development of a successful process for the following: • Laser cleaning of material to give better weld performance using ns green laser. • Laser welding of dissimilar materials (particularly ferrous and aluminium) sheets of between 0.8 and 4 mm using a hybrid system of a CW 1080 nm laser and 515 nm ns pulse laser, or some parameter combination thereof. • Laser cleaning of post-weld material using the same ns green laser. Enabling material transition, setup reduction and a reduction from 15-minute to 5-minute cycle times.
Component	CCB system and its accompanying retainer brackets and attached components.
Illustrations	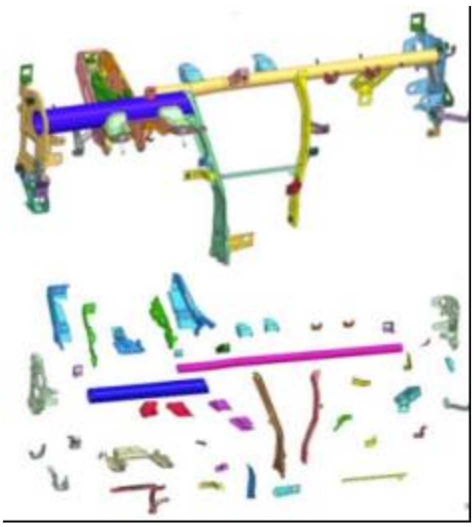

	CCB assemble and exploded view of the assembly
Current manufacturing process	Cutting of steel workpieces from material stock Stamping of sheet metal for brackets Roll forming of steel tubes. Gas metal arc robotic welding to semi-finished state. Manual projection welding of fixtures across three workstations.
Currently used materials	Steel of varying thicknesses and dimensions. (Specific alloys and dimensions unspecified)
CO_2 impact	45g CO_2/100 km decrease in final car emission achieved via a 1.5 kg weight saving. 46.6 CO_2e per annum saving via a 30% reduction in processing cost.
Current energy demands (kg/yr)	No data at present.
Component production /annum	300,000 Cars per annum. 180,000 CCB per line per annum.
Functionality	The CCB is a major structural component of a car providing the necessary rigidity and fixturing of various functional components. The main CCB is joined by welded brackets onto the main structure of the car as well as having subsidiary parts attached via welding. All welds need to be of high integrity to meet stringent structural requirements.
FLASH impact on existing manufacturing and savings	Increase of welding speed from 4 mm/s to 15 mm/s, decrease in cycle time from 900s to 300s per component leading to a cost saving of up to 50% on this process. Reduction in shielding gas usage compared to conventional GMAW. Minimum energy saving of 108 MWh/a when compared to the current welding process.
Processes/Materials to be used with FLASH solution	Laser cleaning using a 515 nm ns pulsed (2-5 ns) laser. Laser welding using a combination of 1080 nm CW and 515 nm ns pulsed laser. Materials to be used include Steel and Aluminium sheets of 0.8 to 4 mm thickness to be welded onto existing thick section rolled stock.

2.3 DePuy Synthes - Manufacturing orthopaedic hip implants

DePuy Synthes is a subsidiary company of Johnson & Johnson, who produce a range of orthopaedic implants for human joint reconstruction and traumatic skeletal injuries. Their product range is one of the largest in this industry and they service a global patient network [23].

2.3.1 Current process and challenge

The acetabular cup is a complex three-dimensional high-precision component that forms a crucial part of an orthopaedic hip reconstruction implant system. The acetabular cup is a modular component, manufactured for various biological and mechanical fixing requirements. This cup provides the accurate positioning of the polyethylene liner, bearing assembly and connection point for the inserted femur stem, as shown in Figure 2-3.

Figure 2-3. Example of the acetabular cup from orthopaedic hip implant system and exploded assembly of the acetabular cup, linear and ceramic bearing head

The cup comprises a titanium alloy shell, with a sintered titanium POROCOAT® coating on its outer dome surface. The current methods for manufacturing the acetabular cups are based on CNC machining of either: a titanium alloy (Ti-6Al-4V) forging, or more recently near-net-shaped additive manufactured bases. In both cases, a minimum of six independent mechanical tool-based operations, listed below, are required to produce the final component. The key functional features are indicated in Figure 2-4.

1. Coarse milling of the inner dome face to required dimensional tolerances.
2. Grinding of the inner dome face to achieve the required surface roughness.
3. Milling of circumferential locking features to required dimensional tolerances.
4. Milling of multiple anti-rotation slots to specified depths.
5. Drilling and tapping of fixturing holes to required diameters and inclinations.
6. Laser marking of text and symbols on the base of the cup.

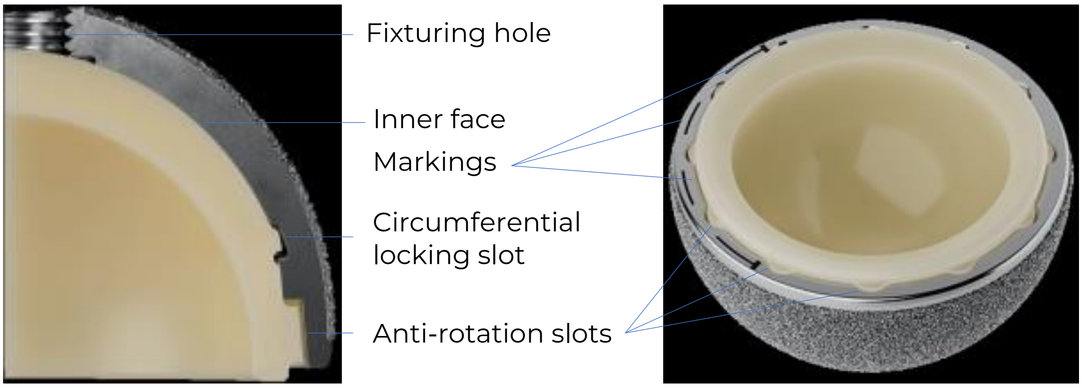

Figure 2-4. Key functional features of the acetabular cup

Current CNC machining operations require expensive tooling, multiple processing steps, high precision fixturing and cutting fluids. Several metrology measurements are taken intermittently during the manufacturing processes to ensure the geometric conformity of the produced parts. This is required due to the high-precision tolerances ranging from 0.01-0.2 mm across the various geometric features of the cup. The inner dome surface which interfaces with the polyethylene liner is ground to a maximum surface roughness (Ra) of 1.6 µm. The addition of the POROCOAT® outer dome coating is applied after all preceding manufacturing processes are completed. This feature is currently being addressed in the SYNTEC project currently funded by the European Commission [24]. Separate conventional laser marking systems are used to finish the production by creating human-readable text and symbols on the various surfaces of the cup. The exact geometry, inclination and relative positions of the various features are defined by the product category and variant (e.g. cup shell sizes range from 44-80 mm in diameter) [25]. The 66 mm diameter Pinnacle Hip Cup is the most widely used. The cup thickness can range between 2-6 mm over the cross-section of the dome.

Current machining cycle times range between 8–10 minutes due to the limited productivity of CNC machining. With additional time required to complete the finishing steps and marking. Between each manufacturing step the shells undergo a multi-stage cleaning and sterilisation process. With 181,808 cups produced per annum, it is vital to reduce the machining cycle times and the need for expensive tooling, whilst maintaining the strict production quality and precision level.

2.3.2 Business and operational requirements

DPS aims to streamline and quicken its acetabular cup production process, whereby a laser-based production tool can machine various cup features with a single machine architecture and at a shorter cycle time. A considerable estimated cost saving is achievable through the adoption of laser-based subtractive manufacturing. This will eliminate an estimated 9,000 mechanical tools and 8,000 litres of coolant per annum from their production facilities. The current consumable cost, including coolant, is estimated at €2.50/part. Part scrap rates with the current manufacturing processes are typically ~10%, with the highest percentage of scrap parts (~30%) due to tool issues (misalignment, breakage, other damage). Elimination of expensive consumables, scrap and rework could deliver €1.1M in annual savings when scaled to multiple production streams and manufacturing sites. The reduction in waste and production by-products will drastically improve the overall sustainability of the DPS production process. The flexibility of the FLASH system that offers multiple laser-based subtractive machining and surfacing capabilities can be used to reduce the requirement for mechanical tool-based processing whilst increasing production throughput rates.

Three independent manufacturing systems (milling CNC, turning CNC and laser markers) are used to produce each acetabular cup. This represents a significant CAPEX burden along with high maintenance and operational costs. A FLASH single-machine architecture that can address most geometric features will reduce the overall number of required systems and their associated costs.

The environmental impact of the production of the acetabular cups results in waste materials such as ~345,000 kg per year of polishing media sludge, ~100,360 kg per year of polishing media and ~2,850 kg per year of titanium swarf generated at a single manufacturing site. FLASH will be able to remove the need for polishing media and reduce the total amount of titanium swarf, leading to a sustained reduction in production waste and CO_2 emissions per implant.

Laser-based production is largely unexploited by DPS, thus their current design philosophy is based on traditional tooling methods. However, the adoption of laser-based manufacturing may lead to a shift in DPS design policies and approach, fostering a "design for lasers" mindset which could lead to savings across their wider product offering and possibly new or improved products.

2.3.3 Approach

DPS's case study will investigate various forms of subtractive laser machining (drilling, cutting, and slotting by WJGL) and laser surfacing (cleaning, marking, and texturing) processes. This use case will deploy all three laser sources and beam delivery methods to carry out the necessary manufacturing processes. In-process monitoring will enable increased traceability and consistency of each manufacturing step along the component's production. The combined AI process optimisation and flexible system will ideally enable the FLASH system to meet the tight tolerances, specifications, and cycle time requirements to be considered as a viable alternative to conventional manufacturing processes. To evaluate and demonstrate this application, the FLASH project will develop laser capabilities to address at least three key features of the titanium acetabular cup bases, these features include:

1. Machining of the fixturing hole at the top of the acetabular shell, with bulk machining with the CW laser and finishing to the required tolerance by WJGL with zero thermal defects.
2. Machining of the various anti-rotational slots to the specified depth using WJGL.
3. Galvoscanner-based short ns laser macro- and micro-polishing, cleaning and texturing of the inner dome surface and marking of identifier features such as human-readable text and symbols.

The representative material that will be used to demonstrate this end-use case will be titanium (Ti-6Al-4V) alloy shell bases which are produced by conventional forging and metal additive manufacturing. The use of an additive shell base may lead to further process step reductions as the bulk laser machining process may be negated and only finishing procedures may be required to achieve the specified tolerances. Cutting operations will be required to produce through-thickness holes of varying diameters and slots to a depth of up to 4 mm. Laser surfacing will be required to achieve an average roughness value (Ra) of 1.6 μm on the three-dimensional inner dome surface.

Laser marking of text, logos, device identification, data matrices and other symbols are all required. Black marking is well suited for this application due to the medical nature of the use case. This method results in superior quality, well-defined marks, with higher contrast, negligible heat impact, substrate structural change and produces higher corrosion resistance. This will be achieved through the deployment of the short, pulsed green ns laser system with beam shaping.

2.3.4 Evaluation methodology

The overall performance capability of the FLASH system will be assessed against existing production methods by DPS. This will consist of assessing each produced feature against the conventional CNC process. An equivalent throughput target rate of 50 parts per machine operation[1] per 12-hour shift is specified for the FLASH system to be considered viable. This will equate to a 50% target of today's total production cost.

The produced components will be evaluated according to the ISO 7206-1 Implants for Surgery – partial and total hip joint prostheses – Part 1: Classification and designation of dimensions. Additionally, DPS will evaluate the overall quality of the produced components according to numerous internal standards. The various machining steps will be assessed primarily on conformity to the specified geometric tolerances, which will be assessed with Coordinate Measuring Machine (CMM) analysis. The results of laser surfacing/texturing procedures will be assessed by profilometry to ensure conformity with the required surface roughness. All test methods will be carried out according to recognised ISO or ASTM standards and within the ISO 13485 Quality Framework.

2.3.5 Case study summary

Table 2-4Table 2-2 lists a key summary of the DPS end-use case.

Table 2-4. Summary of DePuy Synthesis end-use case

Case study	Machining of acetabular hip cups.
Challenges	Developing laser-based manufacturing processes for complex acetabular cup production, replacing current CNC machining process to achieve cycle time reduction, decreased scrap rate, cost and environmental savings.
Objectives/ KPIs	• Replace multiple operations/machines with a single station for machining and marking. • Lower total machining time from 10 minutes to 5 minutes per component. • Reduce scrap rate from 10%. • Decrease in quantity of waste material from process.
Component	Orthopaedic hip implant

[1] A single machine operation includes both the manufacturing process and inspection.
Machine Operation 1: Bulk machining by 5-axis CNC with CMM conformity inspection.
Machine Operation 2: Finishing by milling/turning with CMM conformity inspection.

Illustrations	 Acetabular cup, polyethylene liner & ceramic head 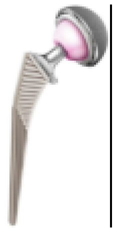 Total hip implant system
Current manufacturing process	High-precision 3D CNC machining. • Coarse turning of the inner face. • Fine turning of inner face to tolerance. • Milling of anti-rotational slots. • Custom Profile tool for drilling holes.
Currently used materials	Ti-6Al-4V alloy and sintered titanium coating. The thickness of the material varies from 2 – 6 mm over the geometry of the component.
CO_2 impact	No data is provided at present.
Current energy demands (kg/yr)	345,000 kg/yr polishing media sludge, 100,360 kg/yr polishing media, 2,850 kg/yr titanium swarf.
Component production /annum	181,808 cups/annum.
Functionality	The cup component directly faces the existing bone structure and provides the seat for the liner. Anti-rotational slots and holes are functional features. All features have high tolerance requirements for implant performance and lifespan.
FLASH impact on existing manufacturing and savings	Financial savings from FLASH is 50% of today's total cost, from a combination of reducing machining cycle time from 8-10 min to 4-5 min and a reduction in consumable cost from ~€2.50/part and a reduction in scrappage rate from 10%.
Processes/Materials to be used with FLASH solution	Ti-6Al-4V The FLASH system will reduce the number of CNC and laser marking systems and operations. Utilizing all three beam delivery heads and at least two laser sources.

2.4 Diamoutils - Advanced tooling of micro-drills and abrasive grinding wheels

Diamoutils is an advanced tooling manufacturer, that produces industry-leading super-abrasive cutting, grinding, and super-finishing tools. DIA advanced tools are used extensively in aerospace, automotive, bearing, medical, and sports equipment manufacturing [26].

2.4.1 Current process and challenge

The current processes for DIA to produce microdrills, shown in Figure 2-5, start with the production of Tungsten Carbide (WC) drill shanks. These are produced via mechanical grinding to achieve the final shape. The shanks are then coated in poly-crystalline diamond (PCD) via chemical vapor deposition (CVD). However, the coatings can fail because of limited adhesion between the layers. This can result in PCD tools often failing to reach the desired ten times increase in tool life over conventional WC tools. The challenge here is that while it is possible to sinter diamond onto the WC tool shank, there is no way to process that effectively using mechanical machining because of the hardness of the diamond [27].

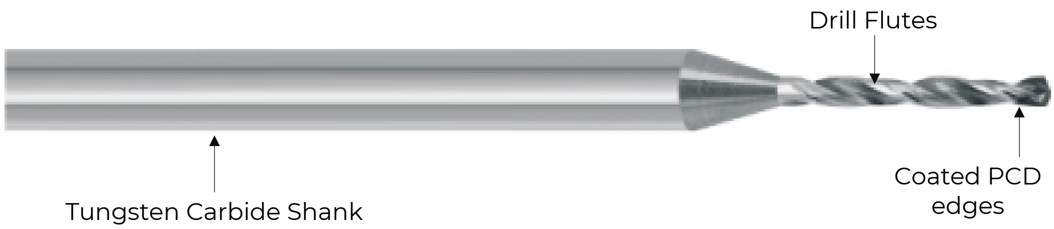

Figure 2-5. Example of the polycrystalline diamond micro-drill bit

Laser processing for PCD is an area that has been explored to overcome these challenges using short-pulsed lasers to achieve machining and texturing of PCD substrates [28] [29] [30]. This has significant advantages for working with PCD compared to other means of processing, such as the ability to create functional textures that improve cutting performance [31] [32] and a reduction in the heat-affected area compared to processes such as Electrical Discharge Machining (EDM) [33]. Laser machining and surfacing PCDs with short pulse durations (ns and shorter), as will be used in the FLASH system, have better performance than longer pulse duration (CW/ms) alternatives due to the reduction in heat accumulation.

To realise the benefits of the FLASH system, the part challenge to be overcome in this use case will be the ability to perform every material removal machining step required to produce a PCD drill bit. This will include rough shaping of the WC through to applying functional surfaces to the drill flutes. There are also the accompanying challenges to enable further benefits offered by laser-based manufacturing such as manufacturing sub 1 mm diameter drill bits or creating an increased number of cutting edges compared to the conventional processes.

The methodology of producing super abrasive grinding wheels starts with the shaping of the wheel hub. This is followed by attaching the abrasive medium (either PCD or cubic Boron Nitride (CBN)) by galvanic electroplating. This involves a great deal of polluting and hazardous chemicals in which the abrasive particles and coatings are suspended. This can produce a non-uniform abrasive structure on the surface of the wheel. This can lead to clogging or uneven load on the tool, reducing the performance and lifespan of the produced tools.

Laser processing will address these issues by allowing solid material to be processed to form a grinding surface, removing the need for the plating chemicals and process, as well as being able to produce an ordered and designed texture on the surface to improve consistency and hence performance and lifespan.

Laser processing of CBN and PCD for grinding tools has been explored [34] with laser ablation being a feasible process to shape the abrasives. Subsequent applications of texturing of the abrasive materials to improve performance are quite well explored [35] [36]. Laser-textured grinding wheels are expected to improve performance and lifespan by decreasing contact forces and wear on the tool.

The final challenge for this use case in the FLASH project will be similar to that of the PCD drill bit. This will involve the development of a laser-based multi-stage process that can be deployed on a single laser architecture.

2.4.2 Business and operational requirements

Through the FLASH project, DIA is aiming to address several manufacturing and environmental factors to improve its product processes and offerings. The first is that the FLASH machine offers the capability to remove galvanic electroplating cycles currently used in the production of super abrasive grinding wheels. This will result in the removal of the cycle time of that process which can be as long as six weeks. Removal of the galvanic process will eliminate the use of environmentally damaging chemicals and wastes from this production. Directly leading to improved capacity for production on the grinding wheel product line and decreasing its environmental impact.

The next outcome is that it will enable innovative product designs, improving the performance of both the super abrasive grinding wheels and the PCD microdrills. Innovative laser processing can be used to introduce design features such as chip deflection, cooling channels, chip breakers, functional surface textures and shaping of the relevant parts of the surface. Implementation of all of these will provide significant advantages to DIA in enhancing its product range.

The third outcome is that both current production procedures have a significant number of time-consuming steps and changes between machines. For example, four separate setup operations are required in the microdrill production. Condensing this to a single setup will dramatically improve processing time and enable significant increases in throughput.

The fourth is that currently there is a high proportion of waste in both processes, with scrappage rates sitting between 20-30%, a particular cause of this is tool breakage in the machining of the much smaller diameter drills. Switching to a laser process will reduce forces on the workpiece whilst providing greater manufacturing precision. Adoption of a laser-based process is expected to decrease the scrappage rate whilst maintaining quality standards.

The fifth is that FLASH provides the ability to manufacture a batch size of one and respond quickly to changes and opportunities in the market. This is particularly relevant to DIA in the PCB market, where these tools are used on a wide range of materials from metals to glass epoxies. Being able to offer specialised tools for the job and use the FLASH tools to quickly design a manufacturing process for a new specific drill geometry is a promising and unique opportunity.

Current production rates for the drills are 500 per annum and 200-500 per annum for the wheels, the cycle time for a micro-drill is four hours, and the cycle time for a wheel can be as high as six weeks depending on the electroplating process. The improvements in cycle time and decrease in scrappage rates when realised will greatly enable an increase in throughput for DIA.

2.4.3 Approach

The approach to demonstrate the process will be via a test run on equivalent materials as they might be employed in service. A 1 mm diameter drill will be produced using a seven-step process.

1. Cutting of the raw material to the required size using a CW laser.
2. Turning of the drill blank macro-geometry using the WJGL.
3. Precision machining of micro-features and flutes using ns galvoscanner.
4. Cutting edge sharpening using galvoscanner ns laser.
5. Micro-polishing of flutes for enhanced chip removal using the galvoscanner and short ns laser.
6. Texturing of tool edges and flutes for tribological properties using galvo-based ns laser.
7. Shank marking and identifiers using ns laser.

For the super abrasive grinding wheel, an eight-step process will be developed.

1. Mechanical CNC precision profiling of wheel hub.
2. Introduction of appropriate masking material to cover regions of the wheel to prevent adhesion of the abrasive material.
3. Laser drilling/ablating of abrasive pockets to locate abrasive materials using the galvo-based ns laser.
4. Ablation of chip evacuation paths and coolant delivery channels using the waterjet-guided laser.
5. Using an end-user developed vacuum brazing/attachment process (silver brazing or nickel-based powder bond) to adhere the abrasive material within defined locations.
6. Precision truing and dressing of wheel profile using waterjet guided laser.
7. Orthogonal profiling of abrasive shapes using the ns green laser with galvoscanner delivery.
8. Wheel marking and identifiers using ns laser.

The ideal parameters for these processes will be determined by the Design for Laser processing module to be produced as a part of the FLASH project.

2.4.4 Evaluation methodology

Evaluation of the product produced by the FLASH system will be benchmarked against existing production drills by DIA. The equipment will consist of the following for the microdrills:

1. Production CNC drilling machine.
2. Integrated Promicron spike force dynamometer to capture drilling forces and torque.
3. Thermal imaging camera to monitor tool and workpiece temperature.
4. Acoustic monitoring equipment to monitor cutting action.

The test piece will be a CFRP plate of 1 mm thickness, and the following evaluations will be conducted with respect to a multi-hole consecutive drill regime.

1. Wear analysis of drill geometry as it progresses through its service life, this will involve microscopy and 3D profilometry.

2. Sectioning of the workpiece to measure the consistency of the drilling quality as the number of holes increases, checking for defects e.g. delamination, cracking etc.
3. Comparison studies with the same substrate and equipment with a current production drill.

Evaluation of the grinding wheels will be conducted as follows:

1. Production CNC grinding machine.
2. Integrated Promicron spike force dynamometer to capture grinding forces.

The test piece will be a set of workpiece blocks of 100Cr6 steel heat treated to between 62 and 63 HRC and the following evaluations will be conducted over a set of repeated sample grind profiles.

1. Capturing of grinding performance over the lifespan of the grinding wheel.
2. 3D profile measurement of the ground profiles at regular intervals to assess the development of the produced form.
3. Comparison studies with same substrate and other equipment with existing production grinding implements.

The output of this will be a set of validated demonstrators showing the difference in performance between the two production methods and will demonstrate the potential beneficial outcomes of the FLASH system for this production application.

2.4.5 Case study summary

Table 2-5Table 2-2 lists a key summary of the DIA end-use case.

Table 2-5. Summary of Diamoutils end-use case

Case study	Manufacturing of PCD microdrills and CBN/PCD super abrasive grinding wheels
Challenges	Development of a laser process to produce high hardness PCD tooling and replace existing multi-stage and high tool wear processes. Development of a laser process to produce super abrasive grinding wheels with uniform finish via texturing to replace the existing galvanic electroplating process.
Objectives/ KPIs	1. Develop a laser-based production process suitable for PCD micro drills and super abrasive precision grinding wheels. 2. Reduce material waste by up to 20% in manufacturing micro drills and 30% in super abrasive grinding wheels. 3. Eliminate the need for polluting chemicals used in the electroplating process. 4. Increased surface quality of super abrasive grinding wheels leading to at least a three times increase in service life.
Component	1. Polycrystalline diamond micro drills 2. Cubic Boron Nitride / Diamond grinding wheel

Illustrations	 Polycrystalline Diamond (PCD) microdrill
	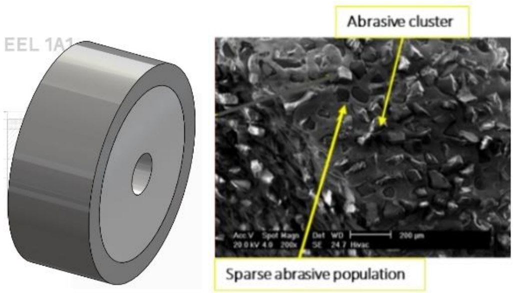 Schematic of CBN grinding wheels and example of abrasive non-uniformity on wheel surface
Current manufacturing process	PCD micro-drills are currently produced by sintering a layer of PCD onto tungsten carbide shanks along with brazing under gas. The Shank profile is machined by multi-axis and multi-stage CNC-Electro Discharge Grinding (EDG). Super abrasive grinding wheels use galvanic electroplating to attach abrasive materials such as CBN or diamond to pre-formed grinding wheel hubs.
Currently used materials	Micro-drills: PCD (cutting layer) with Tungsten Carbide (substrate). Super abrasive grinding wheels Cubic Boron Nitride / Diamond (abrasive layer), substrate (steel or aluminium).
CO_2 impact	No data was provided.
Current energy demands (kg/yr)	No data was provided.
Component production /annum	500 drills/annum in various sizes. 200 – 500 wheels/annum
Functionality	PCD drills are used for micro-hole drilling in PCBs in integrated circuit manufacturing. Precision holes are critical for modern dense circuits. PCD is an ideal material owing to its high hardness, wear resistance and thermal characteristics. Super abrasive grinding wheels are used for precision grinding of hard metals and ceramics in aerospace, automotive and medical. Their output is high levels of precision and control of the final finish. CBN has high hardness, thermal stability and abrasion resistance, whereas

	diamond is sustainably producible with CVD and high-temperature synthesis.
FLASH impact on existing manufacturing and savings	Flash will reduce tool breakages of small-diameter drill components and increase production throughput. It will allow the production of new drill geometries and textures to increase performance. It is aimed to reduce waste by 20% and increase tool lifetime. The laser production of super abrasive grinding wheels will remove the need for polluting electroplating processes, eliminating several hazardous chemicals and overall waste by 30% and enhancing tool performance and lifespan.
Processes/Materials to be used with FLASH solution	PCD microdrills 1. Rough cutting of raw material using CW/ms laser. 2. Fine machining of macro-geometry using ns laser. 3. Precision microgeometry machined using ns WJGL. 4. Cutting edge sharpening, flute micro-polishing and tool texturing using galvoscanner ns laser. Super abrasive grinding wheel: 1. Profiling of hub using CW/ms laser 2. Dimpling of the abrasive site using galvoscanner ns laser 3. Vacuum sintering of abrasives to the site using nickel-based power bond. 4. Profiling of abrasive shapes, ablation of chip evacuation paths and truing/dressing of wheel using ns WJGL 5. Wheel marking using ns laser

3 FLASH system specification

This section of the report outlines the initial specification of the FLASH system and the general components to be integrated with the produced machine platform. It will aim to provide context to the role and functionality of each component, the end-user application-specific definition, the general interface and the interconnection between each component. This portion of the deliverable is associated with T1.1 - Review case studies and refine detailed system requirements and T1.5 - Refine specifications for the system and confirm modifications.

3.1 Components definitions

This section presents the functionality and general specification of components that will be integrated into the FLASH system. It will provide a better understanding of the component's role, operation, and contribution to the overall system and project.

3.1.1 Laser sources

The laser sources are instrumental in the success of the overall FLASH system. These lasers are the functional tools that perform the various laser-based manufacturing processes on the workpieces. In the initial version of the FLASH system, three individual laser sources will be integrated, a continuous wave NIR fibre laser (1080 nm), a green short-duration nanosecond fibre laser (<10 ns and 515 nm wavelength), and a green long-duration nanosecond Diode-Pumped Solid-State (DPSS) laser (~100 ns and 515 nm wavelength). The selection and specification of each of the lasers has been made to provide key processing capabilities within the FLASH system. Table 3-1 lists the key specifications of the lasers and their broad application areas [37] [38] [39].

Table 3-1. General specifications of laser systems

	CW NIR fibre laser	**Green short-duration ns fibre laser**	**Green long-duration ns DPSS laser**
Laser source	Raycus 6000X	IPG GLPN-500-1-50-M	Photonics Industries DM1-527-40
Average / Peak Power	6000 W	50 W	70 W at 10 kHz
Wavelength	1080 ±5 nm	515 nm	532 nm
Mode of operation	Continuous wave / modulated	Pulsed	Pulsed
Pulse duration	-	10 ns	~300 ns at 6 kHz
Repetition rate	Max modulation frequency 2 kHz	10 - 1,000 kHz	1 - 10 kHz
Manufacturing processes	Machining Welding	Machining Surfacing Welding WJGL machining	WJGL machining
Consortium provider	Prima/Cailabs	MTC	Synova

As defined in the above table, each laser source can be used to address various laser-based manufacturing processes required to achieve the end-use case applications. Most critically, the combination of the various lasers will also enable simultaneous multi-wavelength, multi-operational mode (CW or pulsed) processing which is on the cutting edge of modern laser-based manufacturing. Special consideration needs to be given to the optical components due to the application of multiple wavelengths and the wide range of operational powers. This may include careful consideration of the damage threshold of optical components and specialised coatings to ensure the full flexibility of the FLASH system.

3.1.2 Multi-laser fibre coupling module and fibre switch

The integration of the three individual lasers is one of the key impacts of the FLASH system. This will be achieved by developing a bespoke beam combiner, fibre coupling module and single beam output optical system. This optical arrangement will be produced on a single breadboard arrangement with all necessary safety precautions built into the final system. Development of this unit will be led by Synova, who are supported by Cailabs, Aimen and Prima. This system will be developed as part of Work Package (WP) 2. Figure 3-1 provides a proposed configuration of the beam-combining optical system relative to the input lasers and beam delivery units. This beam-combining system also forms the key interconnection between the laser sources and the beam delivery units (nozzle, galvo-scanner and WJGL head). This approach will enable the delivery of at least two of the lasers concurrently in multi-pulse regime beams (NIR CW with short ns or short ns with long ns) through a single-beam delivery method. This significant advancement will unlock entirely new dual laser processing capabilities using, for example, one processing beam and one cleaning beam or co-axial delivery of a multi-wavelength beam. No fibre cables are used between the three distinct units to reduce the cost and complexity of the overall optical system. Additionally, this maintains the beam quality. Individual fibre cables will connect each of the beam delivery units to the fibre switch module.

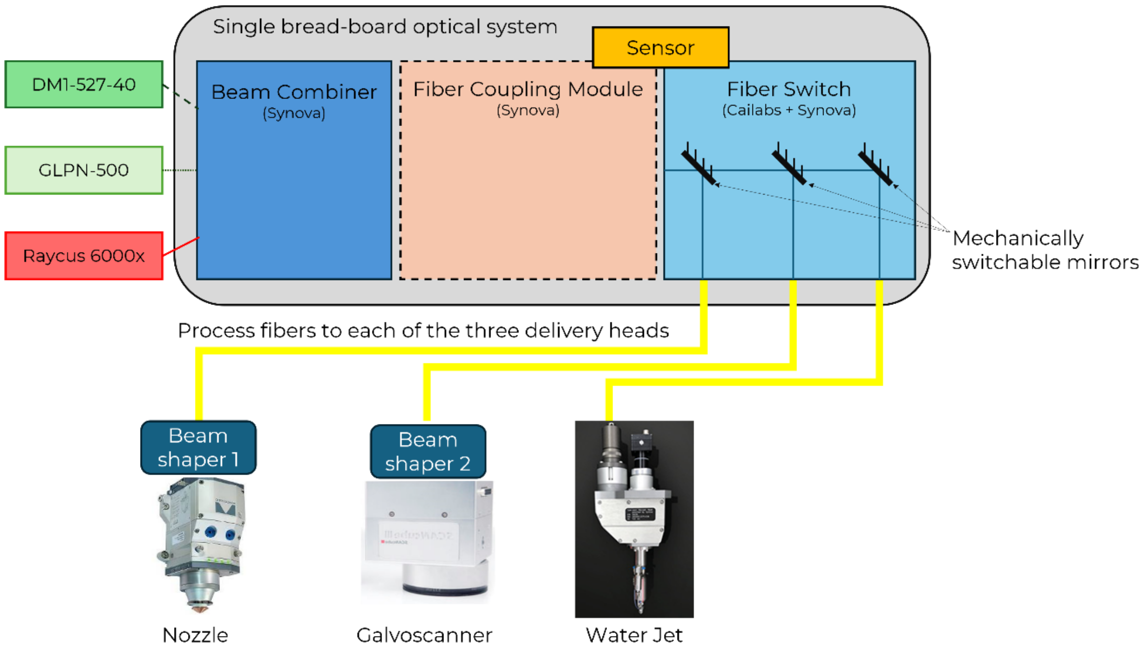

Figure 3-1. Schematic of laser optical architecture deployed in the FLASH system

The Fiber Coupling Module (FCM) will be developed by Synova and will be based on their current commercially available coupling units. This modified system will be adapted to receive the three lasers that operate in the two wavelength types (NIR and green). The beam within the FCM will be under free space propagation. This unit will consist of a combination of off-the-shelf optical elements which will be customized and arranged to meet the Flash specification (wavelength angles, polarisation etc.). The green laser units have different wavelengths, polarisation, and are not coherent with each other. As such, a custom beam splitter and steering mirrors will be required to enable the combination and coaxial alignment of the beams. The same approach will be applied to the NIR beam. Once aligned coaxially, the beams will be positioned into a single output beam that will feed directly into the Cailabs fibre switch.

The fibre switch module, which will be developed by Cailabs, will correctly orientate the single beam output of the FCM to the desired beam delivery unit (nozzle, galvoscanner or waterjet). The beam propagation within the switch will be under free space conditions. The switching unit will use three electro-mechanically driven mirrors to direct the beams. The mirrors will enable the laser beam to either pass unaffected (when in a horizontal position) to the next mirror or to be fully reflected into the dual-core fibre of the selected beam delivery unit. The selection of either mirror will define a singular propagation path to one of the beam delivery units. The configuration of the switch limits the Flash system to only operate a single beam delivery unit at a time. The mirrors will be specifically designed/specified to enable multi-wavelength capability. To achieve a high coupling rate, the mechanical repeatability of the switch will be essential. High-performance switching will be achieved by enacting specific developments in terms of the depointing of the beam. The selected/reflected beam will be aligned and focused into a dual-core fibre cable, the NIR wavelength will be carried in the outer core whilst both green wavelengths will be carried in the inner core. These fibres will be used to direct the beams to each of the delivery units. Besides the 3D beam shaping units, discussed in the next section, on the nozzle- and galvo-based fibre lines, conventional collimation and focusing optics will be used in combination with these beam delivery units. The WJGL delivery unit will not utilise beam shaping. Additionally, the use of the NIR laser with the WJGL delivery will be limited to prevent damage to the internal components of the WJGL head.

3.1.3 Laser beam shaping and focus shifting

Three-dimensional dynamic beam shaping with concurrent adaptive energy distribution of both the green and NIR wavelengths will enable the wider system flexibility and processing capability of the final Flash system. Unlike most conventional laser systems, the Flash system will be capable of dynamically changing its X-Y energy distribution and shifting its Z-plane focal position in response to changing process conditions. This unique functionality will deliver improvements in product quality and process efficiency. Figure 3-2 provides an example of possible three-dimensional beam shapes that are likely to be achieved through X-Y-Z modulation. The shape and position of the beam relative to the workpiece are major factors in determining the laser-material interaction and the success of the process [40]. Additionally, different processes require different energy distributions/shapes, whilst processing complex component geometries consistently is achievable by maintaining the focal length through beam focus shifting.

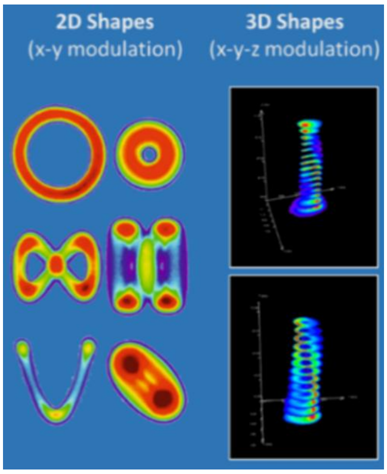

Figure 3-2. Example of dynamic three-dimensional laser beam shapes [40]

X-Y beam manipulation will be achieved by the Multi-Plane Light Conversion (MPLC) unit developed by Cailabs. MPLC achieves free-form beam shaping by passing an incoming beam through a succession of phase plates that are separated by a particular propagation space to control the light's spatial properties (intensity and phase). Figure 3-3.a provides an example of Cailab's current commercial CANUNDA-HP XY beam shaping unit that operates on the MPLC principle. This provides the capability of producing complex beam shapes, such as separate or asymmetrical shapes, or small or large top-hat profiles, some examples are shown in Figure 3-3.b [41] [42]. Laser-induced heating of the optics is largely negated as this MPLC process implements a fully reflective design. This enables the safe use of high-laser powers without large power losses or focus drifts. The Flash beam shaping units will be designed to achieve a dynamic response target time of approximately 10 ms.

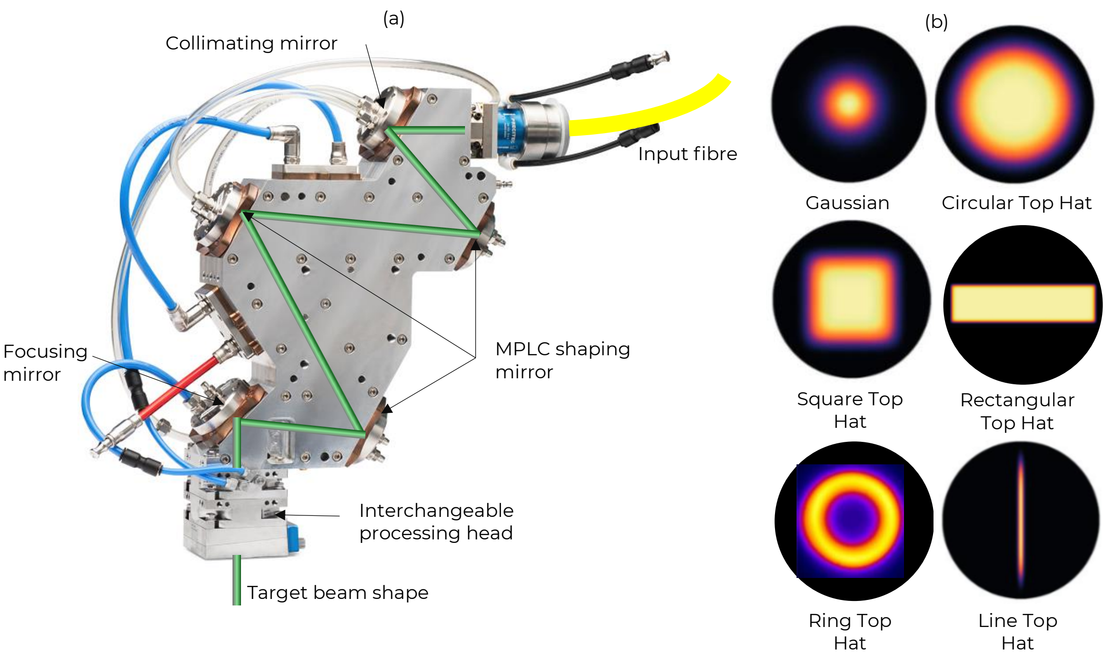

Figure 3-3. (a) Cailab CANUDA-HP beam shaping unit, (b) example of possible laser beam shapes to be generated by the Flash beam shaping unit [41] [42]

A bespoke MPLC system will be developed for the Flash system based on Cailabs CANUNDA concept. Two individual beam shaping units will be deployed on the Flash system, one for the nozzle-based delivery unit and one for the galvo-based delivery unit. Each delivery unit will be attached to the end of the MPLC unit, as indicated by the interchangeable processing head in Figure 3-3.a.

The ability to shape two different wavelengths in a single optical design is a significant challenge. This will be overcome in the beam coupling unit, described in section 3.1.2. However, if this is unsuccessful, wavelength separation will be applied before shaping, with the shaped beams recombined later along the optical pathway.

Focus shifting, Z-position manipulation will be included to achieve a fully three-dimensional dynamic beam-manipulation capability. This functionality will be achieved using a single deformable mirror surface in place of the 90° deflection mirror used at the end of the optical pathway in the delivery head, the location of this optic can be seen in Figure 3-3.a. This focus-shifting unit will be adapted to match the mechanical and optical interfaces of the beam-shaping units and the beam delivery heads. This technology will be provided by Robust AO and is based on their commercial offering of the Zwobble [43]. Figure 3-4 provides an example of the current Zwobbel head that will be adapted for the Flash system [43]. The Zwobbel consists of a membrane within a rigid elliptical frame. The membrane has a mirrored layer, on top of an actuator layer, that can deform the mirrored membrane (piezoelectrically-driven) to adjust the curvature of the surface, thereby shifting the focal position of a laser beam along a single (Z) axis. This design delivers dynamic focus position shifting of up to 20 mm in 2 ms, as shown schematically in Figure 3-4 [43].

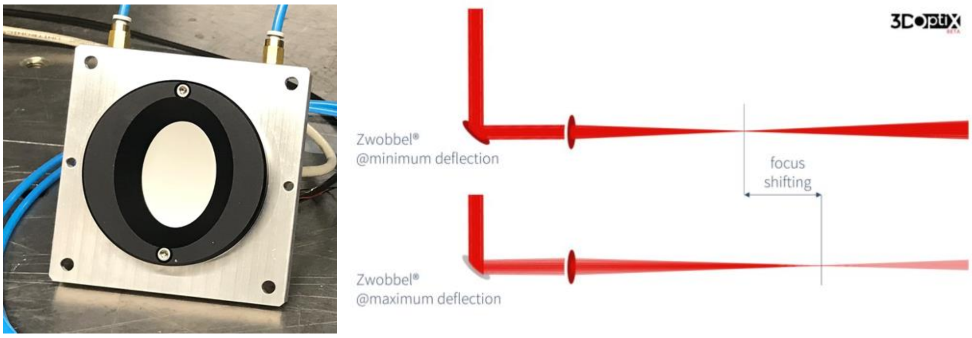

Figure 3-4. Example of Robust AO Zwobble Z-shifting Unit [43]

3.1.4 Laser beam delivery

The Flash system will benefit from three distinct beam delivery units, (1) nozzle, (2) galvo-scanner, and (3) water jet guided heads. Each of these delivery heads will be used to enact the various laser processing capabilities (machining, joining, and surfacing) required by the system. These beam delivery units will be placed at the end of the optical pathway, with all preceding beam manipulation carried out upstream, as shown in Figure 3-1. The nozzle and galvoscanner delivery heads will be specified and modified to deliver both wavelengths (515 & 1080 nm) and laser operational modes (CW or ns-pulsed). Meanwhile, the WJGL head will only be able to operate with green wavelength laser systems. Cailabs will modify a state-of-the-art nozzle and galvoscanner to align with the Flash system architecture. The WJGL head will be developed based on Synova's commercially offered WJGL head [44]. All three units will be fully integrated into the Flash system enclosure. Figure 3-5 provides examples of the three beam delivery units that will be deployed in the Flash machine platform [45] [46] [47].

Beam delivery unit selection will be achieved with a reconfigurable universal docking station. This will be developed in the Flash project and will be used to attach the various beam delivery units to the six-axis robot arm within the enclosure. This

Co-funded by the European Union

docking station will be used for automatic delivery head changeover of the beam delivery head within a few minutes.

(a) Co-axial Nozzle (b) Galvoscanner (c) Water Jet

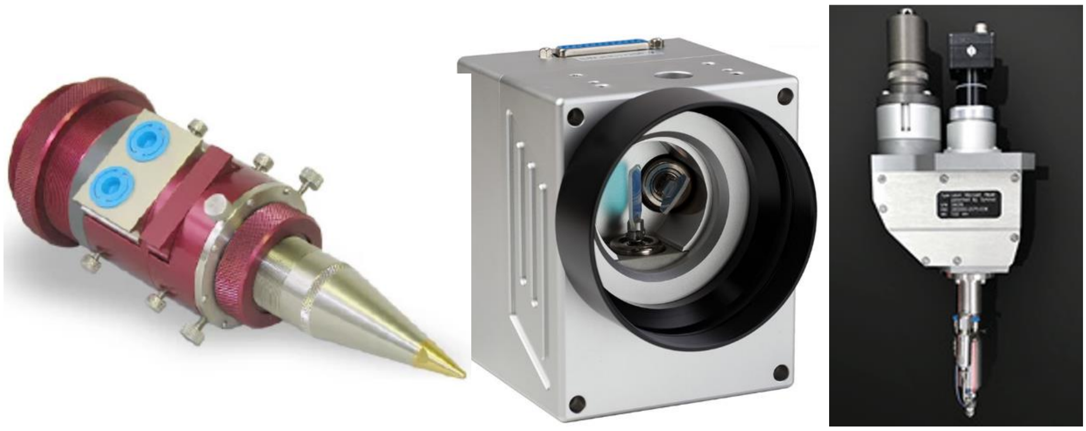

Figure 3-5. Examples of (a) coaxial nozzle [45], (b) galvoscanner [46], and (c) water jet-guided [47] beam delivery units deployed in the Flash system

The nozzle-based delivery system is a commercially available unit that Cailabs will modify to enable safe operation with multiple wavelengths. The nozzle system will primarily be used for cutting, drilling, and welding operations. The nozzle's modular design enables the assembly of custom nozzle tip geometries, and stand-off distances specific to each application. A high-pressure co-axial gas jet of either argon, nitrogen, or oxygen will be applied to improve processing. The nozzle exit diameter will likely range between 1-4 mm. The stand-off distance of the nozzle will be set as per the application by adjusting the nozzle length using the screw mechanism. A focal lens will be incorporated into this unit, with a fixed focal distance in the region of 150-200 mm being selected for the final Flash system. A collimator of a similar range will be specified to achieve the desired beam sizes. This will be defined in succeeding optical and process development work packages.

The galvoscanner will also be adapted based on a commercially available unit to accommodate multi-wavelength processing. This will be achieved by specifying the internal optics and coatings to accommodate the two wavelengths. This device will be used to move the laser beam rapidly and precisely across the target surface through fast reflection of two low inertia mirrors, which can be seen in Figure 3-5.b. This enables the movement of the laser beam at speeds of up to a few meters per second. This delivery unit will be used primarily for fine machining, welding, and surfacing applications. The aperture size of the scanner will be maximised, enabling the largest processing area capability. A 255 mm focal length f-theta lens will be used for this delivery head, providing a flexible working distance. As previously, the collimation lens will be specified based on the allowances of the selected galvoscanner and processing requirements.

The WJGL head will be developed by Synova and is based on their commercial systems, as shown in Figure 3-5.c. Unlike, other delivery methods, the WJGL combines a laser with a high-pressure thin water jet, as shown in Figure 3-6. This completely encapsulates the laser within the water jet by internal reflection, enabling a wide range of material thickness processing (0.01-20 mm). This delivery unit will be used for rough and fine machining of various features of the end-use cases. A secondary water purification and pump system will be supplied with the Flash system. This unit removes any impurities before processing from the mains supplied water, resulting in less chance of water jet breakdown or disturbance. The water pump continuously supplies the nozzle cavity with the purified water at a working pressure between 50-800 bar. Several sapphire-based nozzles, with different aperture diameters ranging between 25-100 µm provide the outlet for the high-pressure jet. The nozzle size will be selected based on the machining application being carried out. As part of the universal docking enclosure, a water jet catcher system will be integrated to terminate the jet when the head is not in use. Critically, a calibration unit for 3D jet detection and jet angle correction will be integrated with the head to enable six-axis machining.

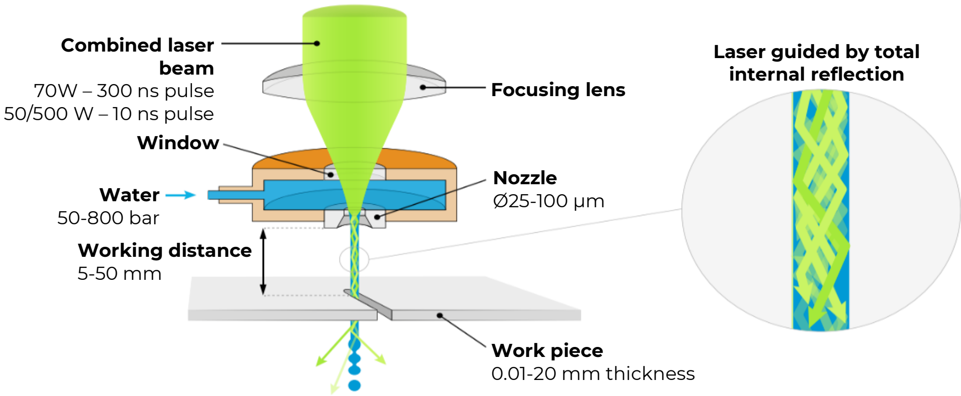

Figure 3-6. Schematic working of the water jet-guided laser process [47]

3.1.5 In-process monitoring

Optical and acoustic sensors will be integrated into the Flash system to develop in-process monitoring and control solutions. This combination of sensors is the most appropriate for in-process monitoring of the full range of processes targeted by the Flash laser platform. The combined optical and acoustic sensor data, processed through a smart data management system will enable rapid process optimisation loops over the full range of laser and kinematic parameters. This delivers the capabilities to maintain a stable, repeatable, and unsupervised manufacturing process.

The optical monitoring system is based on Synova's automatic breakthrough detection sensor [44], will be developed by Synova and AIMEN. This photodiode sensor, mounted co-axially within the beam path, identifies the moment the laser makes the required material-laser interaction by monitoring optical signals reflected from the workpiece. The modified Flash monitoring system will consist of four photodiodes, a spectrometer unit and associated optics, to enable the measurement of emitted light via back reflection. The resulting optical sensor will be mounted inside the optical fibre coupling unit, allowing it to be completely independent of whichever processing head is in operation. The emitted light will pass through a specifically designed optical pathway to segregate the beam for further analysis by optical spectrometry for "slow" analysis and into a bank of four photodiodes for "fast" analysis. Specific coated optics paired with an individual photodiode will provide a near real-time assessment of the intensity of each laser fundamental wavelength, plasma emission and infrared signature, providing a quantitative analysis of the laser/material interaction. The general configuration of the spectrometer and photodiode arrangement are schematically represented in Figure 3-7.

Although acoustic monitoring of laser processes has been widely demonstrated, it is not frequently implemented due to the complexity of the acoustic emissions generated by the laser-material interactions. Additionally, the quality of the measurement is highly dependent on the sensor's spatial positioning relative to the workpiece. Sensor fusion methods, where acoustic sensors are used in combination with other sensors and analysed by machine learning is quickly overcoming these issues.

Several sets of four high-frequency acoustic microphone sensors with a large dynamic range will be integrated around each processing head. This will allow the monitoring solution to capture and record the full acoustic spectrum of all laser processes. This will enable further disambiguation of optical signals to enable derivation of process intensity and control of the process window. Having four microphones per processing head will enable the acoustic emission to be analysed independently of the laser position and shape and will allow for trilateration of various acoustic signals such as the laser-material interaction or post-processing defect generation. The general arrangement of the microphone sets is represented in the schematic in Figure 3-7.

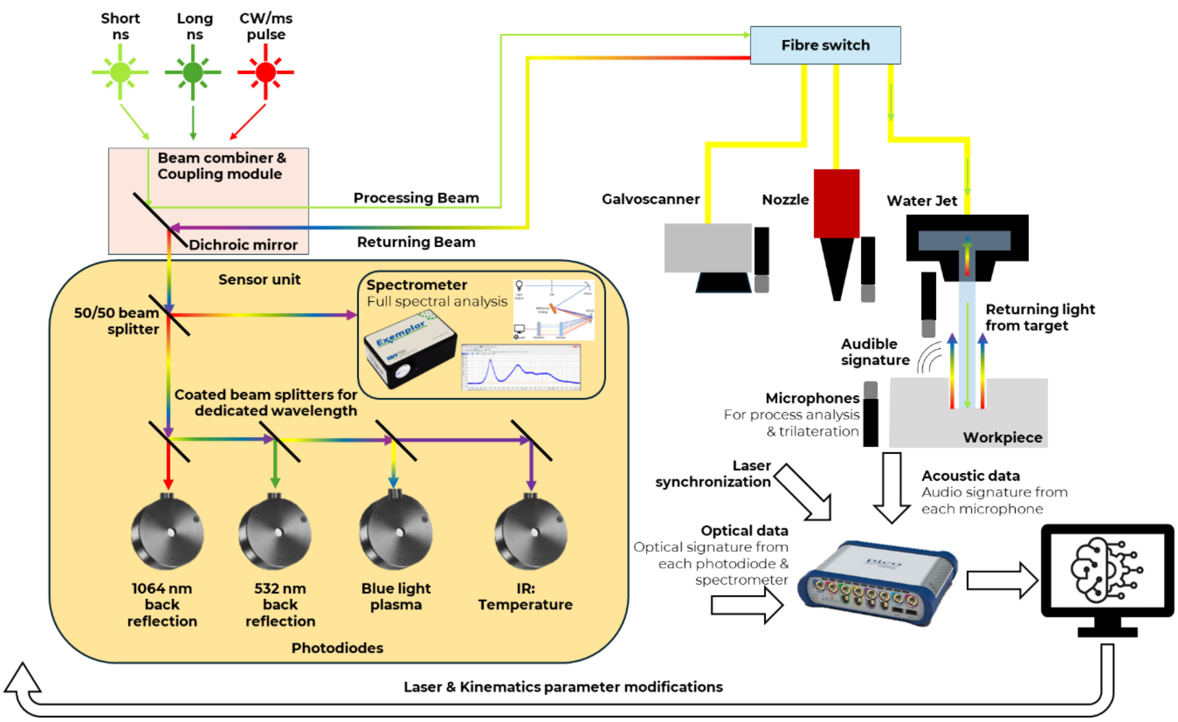

Figure 3-7. Schematic of optical in-process monitoring system

The optical and acoustic signals will be continuously recorded using an eight-channel data acquisition unit. The triggering and synchronization of the lasers will be recorded, providing the exact timing of the various laser processes. The signal data will be processed and analysed in real-time using machine learning algorithms. The analysis will quickly identify any laser process variations. The closed-loop control system will be able to modify the processing parameters (laser and kinematic) to reestablish a stable process and notify users of the processing quality.

3.1.6 Laser system platform

The Flash platform will be based on the Prima IANUS system, shown in Figure 3-8. This is a commercialised 6+2 axis (robotic arm + rotational axis) laser direct energy deposition machine platform. This system can also accommodate other laser-based welding and hardening processes.

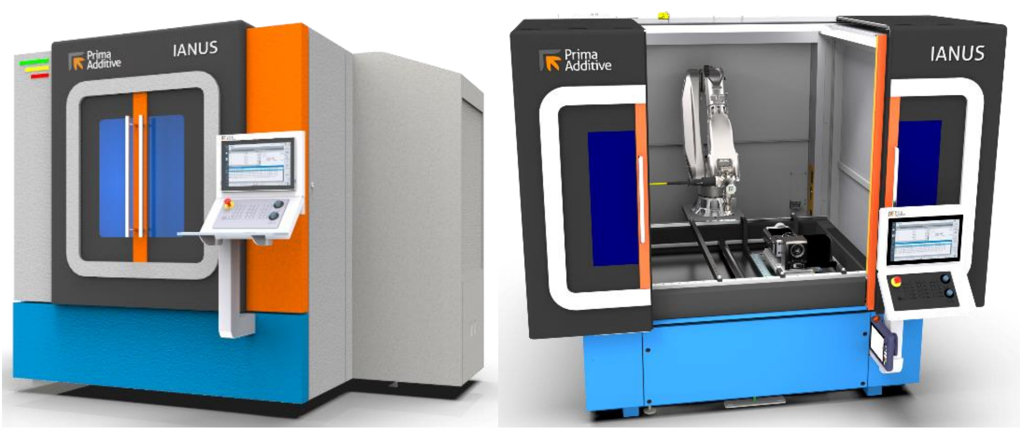

Figure 3-8. Example of the Prima IANUS laser cell

The Flash version of the Ianus system will be re-engineered to accommodate the three individual laser sources and beam delivery methods. Over the project, the enclosure will be developed further to fully incorporate additional kinematic, in-process monitoring, control, and secondary systems to achieve the full functionality of the proposed Flash system. No modifications will be made to the enclosure which may compromise its ability to entirely contain all the planned multi-wavelength laser processes. This will ensure the enclosure maintains its class 1 certification, allowing the system to be operated without the need for operators to wear laser protective safety goggles. An extraction unit will also be coupled with the system to remove processing byproducts such as fumes and fine dust particles. The enclosure will have a working volume of approximately 1600x1200x700 mm but may be reduced to accommodate the additional systems developed throughout the project.

The full kinematics of the enclosure will consist of a six-axis robot arm and a four-axis CNC-controlled axis system. The CNC-axis system will consist of a 360° rotatory, ±120° tilt table, and two 500 mm linear translation stages. The Autonox robotic arm will have a 30 kg nominal payload capacity and an axes speed of 200 °/s (acceleration of 300°/s^2). The two linear axes will be in an X/Y configuration and placed over the B/C axes of the robot. This will provide the complete system with a sub-10 µm positional accuracy and a repeatability of approximately 5 µm within the working envelope. The total system will be able to accommodate components up to a maximum weight of approximately 20 kg and should not be geometrically larger than the specified working envelope of the system. The Flash IANUS system/robotic arm will be fitted with a custom universal docking enclosure/system to facilitate beam delivery head changing (either galvoscanner, nozzle or WJGL). This system will provide the interface to rapidly change the delivery method, providing a tool change operation within a few minutes.

The control of the process parameters and operations will be carried out entirely by the machine systems computerised control system. SINUMERIK One control software, provided by Siemens, will be integrated into the produced Flash system. A SINUMERIK 828 panel-based compact CNC unit will be fitted to allow for control of up to twelve axes and multiple machining channels. This high-performance CNC software is an industry leader for CNC automation and control. In addition, it offers offline programming and efficient post-processing of G-code command machining programs.

Co-funded by
the European Union

4 Process suitability assessment with various FLASH system configurations

The versatility of the Flash system will allow several system configurations to carry out the numerous laser-based manufacturing processes. Table 4-1 outlines the first iteration of laser, beam delivery and beam shaping configurations for each of the anticipated laser processes required to demonstrate the end-use cases. Additional estimates of the quality/cycle capability per configuration have also been provided. Further refinement of the table will be conducted throughout the development of the project. It should be noted that at this stage of the project, the information listed in the table is based on literature and speculation. It is highly likely that this will require further evaluation and may not be fully feasible in the final iteration of the Flash machine platform.

Table 4-1. Specification of broad laser configurations to complete various end-user processes

Key		
 Nozzle	 Galvoscanner	 WJGL
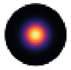 Gaussian	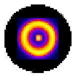 Trident / Ring	 Circular Top Hat

End-user	Applications	Process	NIR CW fibre laser		Green 50W short ns fibre		Green 70 W long ns DPSS		Dual beam	Beam delivery	Beam shaping		Spot size range
			Rough Fast	Fine slow	Rough Fast	Fine slow	Rough Fast	Fine slow			Spatial	Focus shifting	
TOFAS	Prep Fe & Al Comps.	Cut	·	·								·	<50 µm
	Prewelding cleaning	Surfacing			·	·						·	50-150 µm
	Joining components	Join		·		·			·			·	50 - 200 µm

Diamoutils	WC drill shanks (length)	Cut			·	·	·	·	·				25-100 µm based on WJGL nozzle
	Laser turning of WC blanks	Cut			·	·	·	·	·				25-100 µm based on WJGL nozzle
	Drill macro-geometry	Cut			·	·							20-30 µm target
	Drill precision micro-geom.	Cut			·	·							20-30 µm target
	Flute edge sharpening	Cut				·							20-30 µm target
	Flute surfacing (polishing)	Texturing				·							20-50 µm
	Hub wheel truing	Cut			·	·	·	·	·				25-100 µm based on WJGL nozzle
	Dimpling abrasive location	Cut			·	·						·	20-30 µm target
	Profiling abrasive + evac. path	Cut			·	·	·	·	·				25-100 µm based on WJGL nozzle
	Abrasive wheel truing + dressing	Cut			·	·	·	·	·				25-100 µm based on WJGL nozzle
	Wheel marking	Texturing			·	·							20-50 µm
ATOP	Bulk wire skinning	Cut	·	·									50-200 µm
	Residue removal	Texturing	·	·									50-150 µm
	Hairpin joint cleaning	Texturing	·	·	·	·							50-150 µm
	Hairpin joining	Join	·	·	·	·			·			·	50-100 µm inner and 300-350 µm outer ring
DePuy Synthes	Pilot holes – bulk	Cut	·									·	20-50 µm
	Pilot holes – finishing	Cut		·	·	·	·	·				·	20-50 µm
	Slotting anti-rotational slots	Cut			·	·	·	·	·				25-100 µm based on WJGL nozzle
	Surfacing inner surfaces	Texturing			·	·						·	50-150 µm
	Marking of medical comp.	Texturing			·	·							20-50 µm

5 Flash system interface definitions across the consortium

Producing the Flash system will require collaboration between numerous technology and end-user partners within the project consortium. Figure 5-1 outlines the major components of the system and defines the general interdependence between systems. Figure 5-2. lists the primary level functional and integration specifications for the various components within the Flash platform. For clarity, the information for the various components has been presented over two separate tables to improve the table's clarity.

The interfaces between the components have been specified as either mechanical, electrical, optical or software. Other critical specifications have also been specified for increased clarity. Missing data from this table will be expanded upon throughout the project. The purpose of these figures and tables places ownership and clarity for respective partners to deliver assigned components and systems, along with outlining the flow of parts and systems between partners. This will ideally avoid possible issues during the construction of the Flash platform.

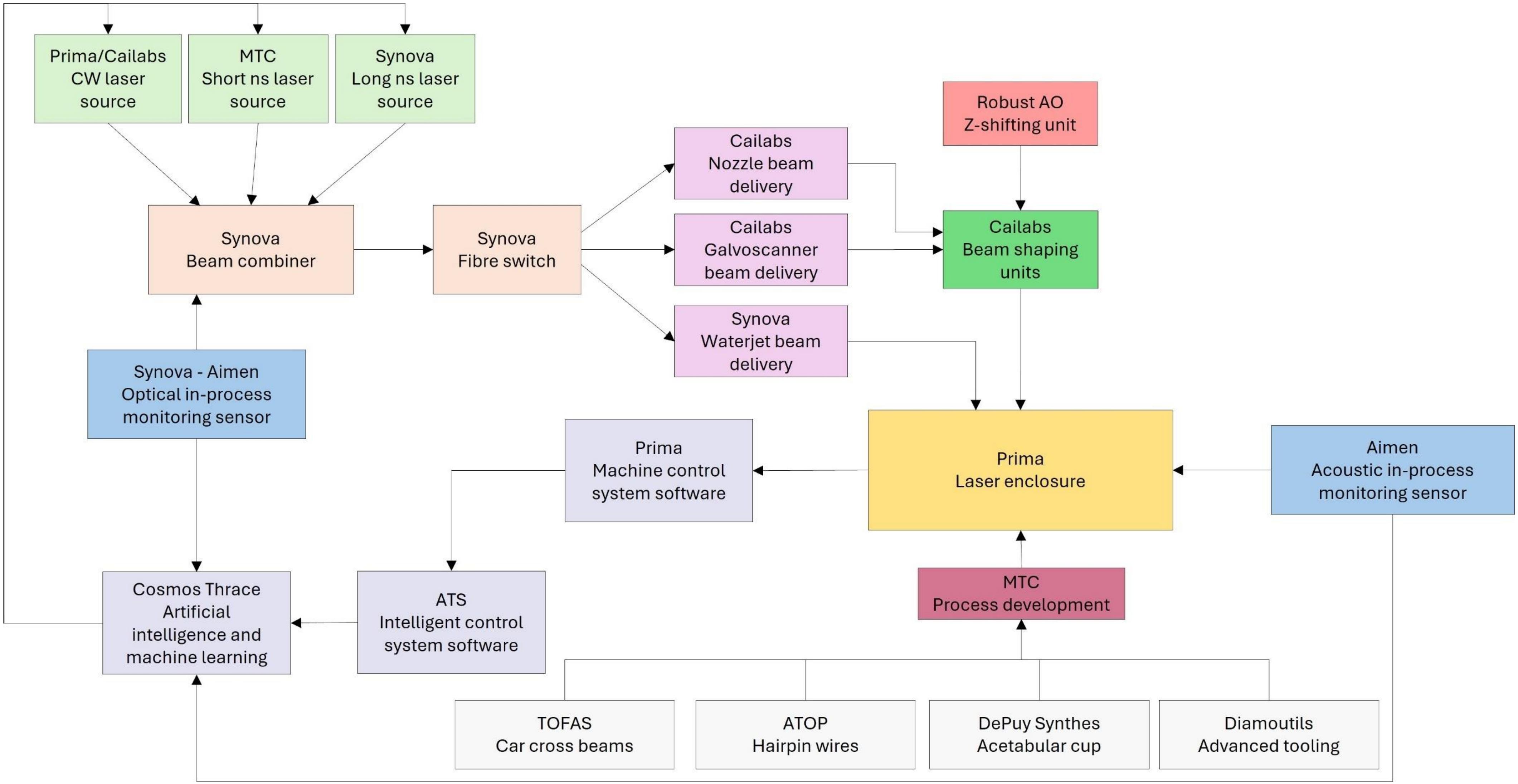

Figure 5-1. Flash system interface diagram

Table 5-1. Summary of component functional and integration specifications

Table one of two.

	Component summary	CW laser	Short ns laser	Long ns laser	Optical in-process sensor	Beam combiner	Fiber switch	WJG beam delivery
	Interface description	**Pri<->Syn**	**MTC<->Syn**	**Syn<->Syn**	**Syn<->Syn**	**Syn<->Syn**	**Syn<->Syn**	**Syn<->Syn**
Responsibility	Shipping	Prima/Synova	MTC/Synova	No shipping	No shipping	No shipping	No shipping	No shipping
	Validation tests	Prima	MTC	Synova	Synova	Synova	Synova	Synova
	Report of validation tests	Prima	MTC	Synova	Synova	Synova	Synova	Synova
	User manual	Prima	MTC	Synova	Synova	Synova	Synova	Synova
Mechanical interface	Dimensions	900x960x1160 mm	264x440x150 mm (module) 65x216x70 (optical head)	661x165x108 mm (laser head) 381x260x89 mm (power supply)	Max. 200x150x50 mm (early estimate)	Unknown (In development)	Unknown (In development)	Unknown (In development)
	Weight	<360 kg	TBC	22.2 kg (laser head) 6.2 kg (power supply)	<15 kg (estimate)	Unknown (In development)	Unknown (In development)	Unknown (In development)
	Cautions	Installation carried out by certified engineers	Installation carried out by certified engineers	Installation carried out by certified engineers	Must be mounted along the optical path of the returning beam	Unknown (In development)	Unknown (In development)	Unknown (In development)
	Fixings	TBC	Module secured with 25 mm m6 screws	Multiple 25 mm, m6 screws	Optical table mounted	Unknown (In development)	Unknown (In development)	Unknown (In development)
	Drawings	Will be provided by Prima	Will be provided by MTC	Will be provided by Synova	Developed during project	Unknown (In development)	Unknown (In development)	Unknown (In development)
Electrical interface	Voltage	Three-phase four wire AC 323V ~ AC 437V	48 V DC	240 V AC	12 V (photodiodes) 5V DC (spectrometer)	Unknown (In development)	Unknown (In development)	Unknown (In development)
	Power consumption	18.5 kW	240 W	TBC	2.5 A	Unknown (In development)	Unknown (In development)	Unknown (In development)

Co-funded by the European Union

	Max current Power supply: Own box/connection or integrated into an electrical cabinet.	TBC	TBC Own connection	TBC Rack mounted own power supply	TBC Standalone power supply per photodiode	Unknown (In development)	Unknown (In development)	Unknown (In development)
	Electrical drawing/connection instruction	Will be provided by Prima	Will be provided by MTC	Will be provided by Synova	Developed during project	Unknown (In development)	Unknown (In development)	Unknown (In development)

Software interface	Protocol of communication	Serial communication / AD	Ethernet	RS232, Ethernet	External trigger, USB	To be confirmed in project	Ethernet	Ethernet
	Table of commands file	To be confirmed in project	To be confirmed in project	Unknown (In development)	Unknown (In development)	To be confirmed in project	To be confirmed in project	Unknown (In development)
	Required inputs	On/off signal Gate signal Laser parameter commands	On/off signal Gate signal Laser parameter commands	On/off signal Gate signal Laser parameter commands	Unknown (In development)	To be confirmed in project	Position of selected laser	General monitoring
	Provided outputs	Laser status General laser monitoring	Laser status General laser monitoring	Laser status General laser monitoring	Unknown (In development)	To be confirmed in project	Selected laser	Water jet status

Optical interface	Output wavelength	1080 nm	515 nm	532 nm	N/A	N/A	N/A	N/A
	Output pulse duration	CW/modulated	10 ns	~130 ns at 1 kHz	N/A	N/A	N/A	N/A
	Output beam size	50 µm	TBC	5 mm @ exit	N/A	N/A	N/A	N/A
	Output max average power	6 kW	50 W	60 W at 3 kHz	N/A	N/A	N/A	N/A
	Output max peak power	6 kW	>150 kW	>300 kW	N/A	N/A	N/A	N/A
	Optical requirements (optics table, contained optics unit, fibre)	Fibre connection between module & head	Fibre connection between module & head	Open air output	Direct input	N/A	N/A	N/A

Cooling system	Type	Water	Air	Water	Air	N/A	N/A	N/A
	Operating temperature range	10-40 °C	15-30 °C	15-30 °C	5-35 °C	Unknown (In development)	Unknown (In development)	Unknown (In development)

Table two of two.

	Component summary	**Nozzle beam delivery**	**Galvoscanner beam delivery**	**Beam shaping units**	**Z-switching unit**	**Enclosure & 10 axes**	**Acoustic in-process sensor**	**Intelligent control system**
	Interface description	**Syn<->Cai**	**Syn<->Cai**	**Cai<->Cai**	**Rob AO <-> Cai**	**Pri<->Pri**	**Aim<->Pri**	**Pri<->ATS**
Responsibility	Shipping	Cailabs	Cailabs	No shipping	Robust AO	No shipping	Aimen	No shipping
	Validation tests	Cailabs	Cailabs	Cailabs	Robust AO	Prima	Aimen	ATS
	Report of validation tests	Cailabs	Cailabs	Cailabs	Robust AO	Prima	Aimen	ATS
	User manual	Cailabs	Cailabs	Cailabs	Robust AO	Prima	Aimen	ATS
Mechanical interface	Dimensions	To be confirmed in project	To be confirmed in project	273x141x64 mm (estimate)	100x100x50 mm (mirror only) 19” 3HE case for electronics	3552x2751x2425 mm	To be confirmed in project	To be confirmed in project
	Weight	To be confirmed in project	To be confirmed in project	2 kg	0.55 kg (+ ~5kg electronics)	3000 kg	To be confirmed in project	To be confirmed in project
	Cautions	To be confirmed in project	To be confirmed in project	N/A	N/A	To be confirmed in project	N/A	N/A
	Fixings	To be confirmed in project	To be confirmed in project	Mounted to robot arm and relative beam delivery unit	Mounted within beam shaping unit	To be confirmed in project	To be confirmed in project	To be confirmed in project
	Drawings	To be confirmed in project	To be confirmed in project	Will be provide by Cailabs	Will be provided by Robust AO	Will be provided by Prima	To be confirmed in project	To be confirmed in project
Electrical interface	Voltage	To be confirmed in project	To be confirmed in project	To be confirmed in project	110-240V AC	400 V AC	To be confirmed in project	To be confirmed in project

	Power consumption	To be confirmed in project	To be confirmed in project	To be confirmed in project	150 W max.	To be confirmed in project	To be confirmed in project	To be confirmed in project
	Max current Power supply: Own box/connection or integrated into an electrical cabinet.	To be confirmed in project	To be confirmed in project	To be confirmed in project	0,5A 2xCEE 7/4 connector for CEE 7/3 sockets	TBC Own connection	To be confirmed in project	To be confirmed in project
	Electrical drawing/connection instruction	To be confirmed in project	To be confirmed in project	To be confirmed in project	Will be provided by Robust AO	Will be provided by Prima	To be confirmed in project	To be confirmed in project
Software interface	Protocol of communication	To be confirmed in project	To be confirmed in project	To be confirmed in project	0-10 V analogue BNC SL2-100 will be provided during the project	Ethernet	To be confirmed in project	To be confirmed in project
	Table of commands file	To be confirmed in project	To be confirmed in project	To be confirmed in project	Commands file will be developed during project	To be confirmed in project	To be confirmed in project	To be confirmed in project
	Required inputs	To be confirmed in project	To be confirmed in project	To be confirmed in project	TBD	To be confirmed in project	To be confirmed in project	To be confirmed in project
	Provided outputs	To be confirmed in project	To be confirmed in project	To be confirmed in project	USB (incl. Software tool)	To be confirmed in project	To be confirmed in project	To be confirmed in project
Optical interface	Output wavelength	N/A	N/A	532/1064 nm	532/1064 nm	N/A	N/A	N/A
	Output pulse duration	N/A	N/A	Same as input	Same as input	N/A	N/A	N/A
	Output beam size	N/A	N/A	Variable	20 mm clear aperture (max.)	N/A	N/A	N/A
	Output max average power	N/A	N/A	N/A	N/A	N/A	N/A	N/A
	Output max peak power	N/A	N/A	16 kW	-pw: LIDT>10 J/cm2 @1030nm, 10ns - cw: 10kW cw (aperture 15mm)	N/A	N/A	N/A

	Optical requirements (optics table, contained optics unit, fibre)	N/A	N/A	Contained optics unit	Contained optics unit	N/A	N/A	N/A
Cooling system	Type	Air	Water	Unknown (In development)	Water	N/A	N/A	N/A
	Operating temperature range	To be confirmed in project	To be confirmed in project	Unknown (In development)	Defined operating temperature range needed (setup between 20-30°C)	N/A	N/A	N/A

6 Conclusion

The development and optimisation of various laser-based manufacturing processes to address the production challenges of the Flash end users will successfully demonstrate the potential of the developed Flash machine platform. The multi-laser and multi-beam delivery system will critically demonstrate the benefits of a flexible high-precision manufacturing solution to the wider manufacturing industry. This will ideally further propel the use of laser-based processes as the global economy shifts towards ever-changing and environmentally conscious manufacturing methods.

This deliverable has summarised the critical aspects of each end-user within the Flash project. KPIs have been defined per end-user, forming the criteria on which the Flash system will be assessed against. Additionally, this deliverable outlines the general details and specifications of the components that will be investigated throughout the remaining WPs of the project. The following summarises each end-use case and its objectives:

ATOP – Improved laser-based cutting and joining by leveraging the deployment of the multi-wavelength system to achieve faster removal rates of the insulating layer surrounding copper hairpin wires. Along with, dual laser welding of hairpin couples for durable, high-strength and low porosity connections.

TOFAS – Development of laser-based welding techniques that are enhanced through beam shaping to enable aluminium-to-steel joining of car crossbeam structures. Key process optimisation is required to mitigate the formation of detrimental inter-metallics that can initiate the premature failure of the components.

DePuy Synthes – Laser machining of key features of a high-precision titanium acetabular cup, based on both forged and additive manufactured blanks. Various laser processes (cutting, drilling, slotting) will be developed to achieve the various geometric features of the component within the tightly specified tolerances.

Diamoutils - Implementing sustainable laser-based manufacturing to produce PCD drill bits and super abrasive grinding wheels. Multiple machining processes which exploit the full capabilities and configurations of the Flash system will be developed to machine, shape and finish numerous features of these advanced tools.

In each of these use cases, the primary objective is to provide alternative cost-effective laser-based manufacturing techniques which aim to reduce process cycle times whilst improving the component's functionality and sustainability.

During Task 1.5, the specifications of the Flash laser machine platform and associated components have been detailed. This provides a clear understanding of the equipment utilised, the integration plan and defining the consortium partner's responsibility for producing the components, equipment or sub-systems. Key components and their specifications include:

1. **Laser sources -** (1) 6 kW CW, NIR 1080 nm fibre laser; (2) 50/500 W, 10 ns pulsed, green 515 nm fibre laser; (3) 70 W, 300 ns pulsed, green 532 nm DPSS.
2. **Beam delivery –** (1) Nozzle-based co-axially applied processing gas with interchangeable nozzle exit diameters and a focal lens of >150 mm; (2) High power multi-wavelength galvoscanner with a >200 mm f-theta lens unit; (3) Water Jet Guided Laser head with interchangeable nozzles ranging from 25-100 µm.
3. **Beam shaping –** Dynamic X/Y spatial beam shaping to produce either Gaussian, Top Hat or Ring beam profiles. Z-positional shifting using reflective multi-

wavelength deformable mirror unit. The three-dimensional dynamic beam shaping unit will be self-contained units that are mounted along the optical path before the nozzle and galvoscanner.

4. **Optical components –** A breadboard-mounted fibre combining unit will used to align the output of each laser source into a singular optical path. This sub-system will be developed in succeeding WPs. An opt-mechanical fibre switching unit will allow for the selection between the three interchangeable beam delivery heads.
5. **In-process monitoring –** Optical and acoustic in-process monitoring systems will be deployed in the Flash machine platform. The optical system will characterise reflected light from the laser-material interface using a spectrometer and a bank of photodiodes. The reflected light will be filtered into its various wavelength components for a full spectrum analysis. The acoustic sensor will consist of high-frequency microphones that are mounted on the beam delivery heads, to record the acoustic emissions during processing. Machining learning will be used to analyse the acoustic and optical signals, providing a real-time measure of any process deviations.
6. **Enclosure and workpiece handling –** The Flash machine platform will be based on the Prima INAUS system. A six-axis robot arm will provide the primary kinematic manipulation, with a four-axis CNC system (two linear translations, tilt and rotation stages) providing increased positional accuracy. A universal docking unit will enact beam delivery changes within a few minutes.

The detailed documentation of the system specification will serve as a valuable resource throughout and beyond the duration of the Flash project.

7 References

[1] I. Automation, "ATOP is part of the IMA Automation Hub," 2021. [Online]. Available: https://imautomation.com/en/news/atop-is-part-of-the-ima-automation-hub-2021-nws-19. [Accessed 05 2024].

[2] S. Arcangelo, L. Caprio, D. Chesi, D. Nocciolini, R. Corbinelli, B. Previtali and A. Demir, "Comprehensive benchmarking of laser welding technologies including novel beam shapes and wavelengths for e-drive copper hairpins," *Optics & Laser Technology,* vol. 169, no. 109964, 2024.

[3] B. Kuntz, "Electric Motor Hairpin Welding: Comparing 3 Joining Technologies," Amada Weld Tech, 2023. [Online]. Available: https://amadaweldtech.com/blog/electric-motor-hairpin-welding-comparing-3-joining-technologies/. [Accessed June 2024].

[4] T. Glaessel , J. Seefried, A. Kuehl and J. Franke, "Skinning of insulated cipper wires within the production chain of hairpin windings for electric traction drives," *International Journal of Mechanical Engineering and Robotics Research,* vol. 9, no. 2, 2020.

[5] K. Kellens, G. Rodrigues, W. Dewulf and J. Duflou, "Energy and Resource Efficiency of Laser Cutting Processes," *Physics Procedia,* vol. 56, pp. 854-864, 2014.

[6] TOFAS, "General Overview," 2018. [Online]. Available: https://www.tofas.com.tr/en/AboutTofas/GeneralOverview/Pages/default.aspx. [Accessed 05 2024].

[7] M. Atabaki, M. Nikodinovski, P. Chenier, J. Ma, M. Harooni and R. Kovacevic, "Welding of aluminium alloys to steels, an overview.," *Journal for manufacturing science and production,* vol. 14, no. 2, 2014.

[8] A. Saai, V. Delhaye, T. Lange, T. Furu, K. Aamon and J. Lein, "Comparitive study of the effects of galvanic corrosion on the strength and failure of aluminium and stainless steel bolted joints," *Journal of advanced joining processes,* vol. 100163, no. 8, 2023.

[9] A. Ruiz-Garcia, V. G. J. Esquivel-Pena and R. Montoya, "Advances in Galvanic corrosion of aluminium alloys," *Electrochemica Acta,* vol. 449, p. 142227, 2023.

[10] A. Sayeed Khan, P. Dong, K. Sun and D. Larsen, "Direct spot joining of thin gauge aluminium alloy to stainless steel and joint performance in a corrosion environment.," *Thin-Walled structures,* vol. 200, p. 111919, 2024.

[11] Institute of Automotive Engineer Assessors, "Warning, JLR Vehicles with aluminium EPAS," 10th March 2021. [Online]. Available: https://www.iaea-online.org/news/2021/03/. [Accessed 6th June 2024].

[12] National Highway Traffic Safety Administration, "Technical service bulletin - Aluminium body panel corrosion repair," NHTSA, Washington DC, 2022.

[13] K. Misiura, J. Konieczny, K. Labisz and R. Boris, "Investigations of the structure and hardness of dissimilar steel to aluminium joints made using laser welding technology.," *Transport Problems,* vol. 17, no. 1, pp. 73 - 86, 2022.

[14] L. Kang, X. C. J. Li, Y. Zhang and T. Wang, "Microstructure and mechanical properties of stainless steel/6082 aluminium alloy heterogeneous laser welded joint," *Materials,* vol. 16, no. 6598, 20203.

[15] T. Li, D.-w. Zhou, Y. You-rui-ling, P. Ping and L. Jin-Shui, "First principles and experimental investigations on ductility/brittleness of intermetallic compounds and joint propertis in steel/aluminium laser welding.," *Transactions of nonferrous metals society of China,* vol. 31, no. 10, pp. 2962-2977, 2021.

[16] C. Zhou, H. Li, G. Chen, G. Wang and Z. Shan, "Effect of single pulsed picosecond and 100 nanosecond laser cleaning on surface morphology and welding quality of aluminium alloy," *Optics & Laser technology,* vol. 127, p. 106197, 2020.

[17] B. Liu, C. Wang, G. Mi, J. Wang, W. Zhang and X. Zhang, "Oxygen content and morphology of laser cleaned 5083 aluminium alloy and its influences on weld porosity.," *Optics and laser technology,* vol. 140, p. 107031, 2021.

[18] P. Wei, Z. Chen, D. Wang, R. Zhang, L. Xinyan, F. Zhang, K. Sun and Y. Lei, "Effect of laser cleaning on mechanical properties of laser lap welded joint of SUS310S stainless steel and 6061 aluminum alloy," *Materials Letters,* vol. 291, p. 129549, 2021.

[19] P. Stritt, C. Hagenlocher, C. W. R. Kizler, C. Ruttimann and T. Graf, "Laser Spot Welding of Copper-aluminum Joints Using a Pulsed Dual Wavelength Laser at 532 and 1064 nm," *Physics Procedia,* vol. 56, pp. 759-767, 2014.

[20] S. Frank, "Flux-Free laser joining of aluminium and galvanised steel," *Jouirnal of Materials Processing Technology,* vol. 222, pp. 365-372, 2015.

[21] Y. Seo, S. Son and D. Lee, "A study of laser cleaning to remove by-products occurring after arc welding," *Materials Chemistry and Physics,* vol. 288, p. 126375, 2022.

[22] Z. Li, D. Zhang, X. Su, S. Yang, J. Xu, R. Ma, D. Shan and B. Guo, "Removal mechanism of surface cleaning on TA15 titanium alloy using nanosecond pulsed laser," *Optics & Laser technology,* vol. 139, p. 106998, 2021.

[23] D. Synthes, "About DePuy Synthes," [Online]. Available: https://www.jnjmedtech.com/en-US/depuy-synthes/about-us. [Accessed 05 2024].

[24] SYNTECS, "SYNTECS - Representative orthopedic implant geometries (Acetabular cup and Hip stem," EWF.BE, 2023. [Online]. Available: https://syntecs-laser.eu/innovation-case-study3.html. [Accessed June 2024].

[25] D. Synthes, *Pinnacle TM hip Solutions Product Catalogue,* 2023.

[26] Diamoutils, "Home," 2016, [Online]. Available: https://www.diamoutils.com/en/. [Accessed 05 2024].

[27] S. Oliaei, Y. Karpat, J. P. Davim and A. Perveen, "Microtool design and fabrication: A review," *Journal of Manufacturing processes,* vol. 36, pp. 496-519, 2018.

[28] F.-Y. Chang, H. Chuan-Fu and W.-H. Lu, "Nanosecond-Fiber Laser Cutting and Finishing Process for Manufacturing Polycrystalline Diamond-cutting tool blanks," *Applied Science ,* vol. 11, no. 13, p. 5871, 2021.

[29] Y. Xia, N. He, L. Z. G. Li, M. Wang and C. Wang, "Study on fabrication of PCD micromilling tool by picosecond pulsed laser," *International journal of Advanced Manufacturing Technology. ,* vol. 105, pp. 4551 - 4557, 2019.

[30] N. Chen, R. Wang, B. Nagarajan, B. Yang, Y. Wu, N. He and S. Castagne, "Investigation of metal-coating-assisted IR nanosecond pulsed laser ablation of CVD diamond," *Journal of materials research and technology,* vol. 18, pp. 4144-4129, 2022.

[31] K. E. Hazzan, M. Pacella and T. L. See, "Laser Processing of Hard and Ultra-Hard Materials for Micro-Machining and Surface Engineering applications," *Micromachines,* vol. 12, p. 895, 2021.

[32] X. Sun, Y. Li, Z. Yu, J. Xu and H. Xu, "Micro-hole texture prepared on PCD tool by nanosecond laser," *Optics and laser technology,* vol. 147, p. 107615, 2022.

[33] G. Eberle, K. Jefimovs and K. Wegener, "Characterisation of thermal influences after laser processing polycrystalline diamond composites using long to ultrashort pulse durations," *Precision Engineering,* vol. 39, pp. 16-24, 2015.

[34] K. Jarosz, E. Ukar, A. Krodel and T. Ozel, “Laser ablation and processing of polycrystalline cubic boron nitride cutting tool material,” *International Journal of Advanced Manufacturing Technology,* vol. 118, pp. 785-800, 2022.

[35] S. Costa, M. Pereira, J. Ribeiro and D. Soares, “Texturing Methods of Abrasive Grinding Wheels: A systematic review,” *Materials,* vol. 15, p. 8044, 2022.

[36] A. Zahedi and B. Azarhoushang, “Microstructuring strategies of cBN grinding wheels,” *International journal of Advanced Manufacturing Technology,* vol. 91, pp. 3925-3932, 2017.

[37] I. Photonics, “Quasi-CW Fiber Lasers,” June 2024. [Online]. Available: https://www.ipgphotonics.com/products/lasers/quasi-cw-fiber-lasers#ftrresources. [Accessed 2024].

[38] I. Photonics, “Green Nanosecond Fiber Lasers,” 2024. [Online]. Available: https://www.ipgphotonics.com/products/lasers/nanosecond-pulsed-fiber-lasers/green-nanosecond-fiber-lasers. [Accessed June 2024].

[39] P. Industries, “DM Green Series Nanosecond Lasers (Multi-Mode),” 2024. [Online]. Available: https://www.photonix.com/product/dm-527-532/. [Accessed June 2024].

[40] A. Jahn, D. Dittrich, S. Börner, J. Standfuss, P. Herwig and C. Reinlein, “3-dimensional beam shaping for dynamic adjustment of focus position and intensity distribution for laser welding and cutting,” in *Lasers in Manufacturing Conference 2021*, 2021.

[41] Cailabs, “CANUNDA HP,” 2022.

[42] Cailabs, “Canunda Pulse,” 2022.

[43] Robust AO, “Zwobbel® fast focusing solutions,” 2024. [Online]. Available: https://robustao.de/zwobbel-fast-focussing-solution/. [Accessed June 2024].

[44] Synova, “LMJ Sensors & Process Control (Industry 4.0),” 2024. [Online]. Available: https://www.synova.ch/technology/sensors.html.

[45] Haas Laser Technologies Inc. , *38 mm G2 "Series" Laser Process Head,* 2024.

[46] BEAMQ, “Galvo Scan Head High Speed Galvanometer Scanner Fiber Laser Marking Machine 1064 nm Sino SG7110 10 mm,” Rock-Solid Laser, 2024. [Online]. Available: https://www.beamqus.com/product/galvo-scan-head-high-speed-galvanometer-scanner-fiber-laser-marking-machine-1064nm-sino-sg7110-10mm/.

[47] Synova, “Laser MicroJet Integration Package,” 2024. [Online]. Available: https://www.synova.ch/products/all-synova-systems/item/66-lmj-ip.html. [Accessed June 2024].

[48] G. Nordet, C. Gorny, Y. D. J. Mayi, M. Dal, A. Effernelli, E. Blanchet, F. Coste and P. Peyre, “Absorptivity measurements during laser powder bed fusion of pure copper with a 1kw cw green laser,” *Optics & Laser technology,* vol. 147, p. 107612, 2022.

[49] D. Wu, J. Sun, Z. Li, J. Huang and K. Feng, “Molten pool behaviors and energy absorption in coaxial hybrid blue-IR laser welding of a copper material,” *International journal of thermal sciences,* vol. 184, p. 107945, 2023.

[50] S.-i. Nakashiba, Y. Okamoto, T. Sakagawa, S. Takai and A. Okada, “Micro-welding of Copper Plate by Frequency Doubled Diode pumped pulsed Nd:YAG laser,” *Physics Procedia,* vol. 39, pp. 577-584, 2012.

[51] A. Blom, P. Dunias, V. Engen and W. Hoving, “Process spread reduction of laser micro-spot welding of thin copper parts using real-time control,” *Procedings of SPIE - International society for Optical Engineering* , vol. 4977, pp. 493 - 507, 2003.

[52] A. Hess, R. Schuster, A. Heider, R. Weber and T. Graf, “Continuous Wave Laser Welding of Copper with Combined Beams at Wavelengths of 1030nm and 515 nm.,” *Physics Procedia,* vol. 12, pp. 88-94, 2011.

[53] M. Pastor, H. Zhao and T. Debroy, “Pore formation during continuous wave Nd:YAG laser welding of aluminium for automotive applications,” *Welding international,* vol. 15, no. 4, pp. 275-281, 2001.

[54] A. AlShaer, L. Li and M. A, “The effects of short pulse laser surface cleaning on porosity formation and reduction in laser welding of aluminium alloy for automotive component manufacture,” *Optics and laser technology,* no. 64, pp. 162-171, 2014.

[55] G. Filliard, M. El Mansouri, L. Tirado, S. Mezghani, C. Bremont and M. De Metz-Noblat, “Industrial fluxless laser weld-brazing process of steel to aluminium at high brazing speed.,” *Journal of manufacturing processes,* no. 25, pp. 104-115, 2017.

[56] G. Yu, S. Chen, Z. W. Z. Zhao, J. Huang, J. Yang and S. Chen, “Comparative study of laser swelding-brazing of aluminum alloy to galvanized steel butted joints using five different filler wires,” *Optics and Laser Technology,* no. 147, p. 107618, 2022.

[57] J. Huang, H. Jing, X. Yu, C. Li and D. Fan, “The study of mechanical strength for fusion-brazed butt joint between aluminum alloy and galvanized steel by arc-assisted laser welding,” *Journal of manufacturing processes,* vol. 25, pp. 126-133, 2017.

[58] L. Li, H. Xia, C. Tan and N. Ma, “Effect of groove shape on laser welding-brazing Al to steel,” *Journal of materials processing technology,* vol. 252, pp. 573-581, 2018.

[59] Y. Shi, L. Jie, Z. Gang, J. Huang and Y. Gu, “Corrosion behavious of Aluminium-Steel Weld-Brazing joint,” *Journal of Materials Engineering and Performance,* vol. 25, 2016.

[60] Z. Sun and J. Ion, “Laser welding of dissimilar metal combinations,” *Journal of Materials Science,* no. 30, pp. 4205-4214, 1995.

[61] K. Martinsen, H. S.J and B. Carlson, “Joining of dissimilar materials,” *CIRP Annals - Manufacturing technology,* no. 64, pp. 679-699, 2015.

[62] N. Ahmed, S. Ahmad, S. Anwar, A. Hussain, M. Rafaqat and M. Zaindin, “Machinability of titanium alloy through laser machining: material removal and surface roughness analysis,” *International journal of advanced manufacturing technology,* no. 105, pp. 3303-3323, 2019.

[63] A. Pramanik and A. K. Basak, “Laser beam machining of Titanium Alloy - A review,” *Metals,* no. 13, p. 1536, 2023.

[64] L. Shanjin and W. Yang, “An investigation of pulsed laser cutting of titanium alloy sheet,” *Optics and lasers in engineering ,* no. 44, pp. 1067-1077, 2005.

[65] I. Almeida, W. de Rossi, M. Lima, J. Berretta, G. Nogueira, N. Wetter and N. Viera Jr, “Optimisation of titanium cutting by factorial analysis of the pulsed Nd:YAG laser parameters,” *Journal of materials processing technology,* vol. 179, no. 1-3, pp. 105-110, 2006.

[66] E. Bektas, L. Subasi, G. Aydemic, J. Diboine, O. Can Ozaner and D. Canadinc, “Water Jet Guided Laser vs. Conventional Laser: Experimental comparison of surface integrity for different aerospace alloys,” *Journal of Laser Micro/Nanoengineering,* vol. 16, no. 1, 2021.

[67] B. Adelmann, C. Ngo and R. Hellmann, “High aspect ratio cutting of metals using water jet guided laser,” *International Journal of Advanced Manufacturing Technology,* vol. 80, pp. 2053-2060, 2015.

[68] Q. Liu, Y. Zhao, J. Meng and Z. Zheng, “Experimental Research and Optimization of Ti-6Al-4V Alloy microgrove machining based on waterjet guided high power laser,” *Materials,* no. 15, p. 7430, 2022.

[69] A. Cavaleiro, C. Fernandes, A. Farinha, C. Gestel, J. Jhabvala, E. Boillat, A. Senor and M. Viera, “The role of nanocrystalline binder metallic coating into WC after additive manufacturing,” *Applied surface science,* vol. 427, pp. 131-138, 2018.

[70] C. Fernandes, V. Ferreira, A. Senos and M. Viera, “Stainless steel coatings sputte deposited on tungsten carbide powder particles,” *Journal of Surface Coating Technologies,* vol. 176, no. 1, pp. 103-108, 2003.

[71] M. Pacella, D. Axinte, P. Butler-Smith and M. Daine, “On the topographical/chemical analysis of polycrystalline diamond pulsed laser ablated surface,” *Procedia CIRP,* vol. 13, pp. 387-392, 2014.

[72] S. D. Dondieu, C. Newson, P. Ghosh, H. Elkington, P. Butler-Smith and S. Marimuthi, “Investigating surface integrity of laser-machined polycrystalline diamond using a 300W picosecond laser,” *7th CIRP{ conference on surface integrity,* vol. 123, pp. 334-339, 2024.

[73] G. Eberle and K. Wegener, “Ablation study of WC and PCD composites uising 10 ps and 1 ns pulse durations at green and IR wavelengths,” *Physics Procedia,* vol. 56, pp. 951-962, 2014.

[74] P. Fernandez-Lucio, I. Villaron-Osorno, O. P. Neto, E. Ukar, L. L. de Lacalle and A. G. del Val, “Effects of laser-textured on rake face in turning PCD tools for Ti6Al4V,” *Journal of Materials Research and Technology,* no. 15, pp. 177-188, 2021.

[75] J. Yin, G. Chen, Z. Huang, C. Chang, X. Yin, Q. Zeng and J. Liu, “Fabrication of PCD face grinding wheel with positive rake angle by femtosecond laser and its performance evaluation in cemented carbide grinding,” *Diamond & Related materials,* vol. 139, p. 110418, 2023.

[76] B. Denkena, T. Grove, A. Krodel and L. Ellersiek, “Increased performance in high speed turning of Inconel 718 by laser structuring of PcBN,” *8th CIRP Conference on High Performance Cutting,* vol. 77, pp. 602-605, 2018.

[77] S. Fang and S. Klein, “Surface structuring of Polycrystalline Diamond using ultrashort pulse laser and the study of force conditions,” *International Journal of Refractory Metals and Hard Materials,* vol. 84, p. 105036, 2019.

[78] O. D. E. Panel, “Pinnacle Cementless Acetabular Cup - DePuy Synthes,” [Online]. Available: https://www.odep.org.uk/product/pinnacle-cementless-acetabular-cup/. [Accessed June 2024].

[79] J. Enz, S. Riekehr, V. Ventzke, N. Sotirov and N. Kashaev, “Laser welding of High-Strength aluminium alloys for the Sheet Metal Forming Process.,” *Procedia CIRP,* no. 18, pp. 203-208, 2014.

[80] L. Cui, H. Chen, B. Chen and D. He, “Welding of Dissimilar Steel/Al Joints Using Dual-Beam Lasers with Side-by-Side Configuration,” *Metals,* vol. 8, no. 2, p. 1017, 2018.

[81] G. Zhu, S. Wang, M. Zhang, X. Yang, W. Liu and G. Wang, “Application of laser cleaning in postwelding treatment of aluminium alloy,” *Applied Optics,* vol. 59, no. 34, pp. 10967-10972, 2020.

[82] L. Barreto, M. Mashhadikarimi, M. Rodrigues, D. Gurgel, U. Gomes, M. Filgueira and R. Medeiros, “Preparation and characterization of sintered polycrystalline diamond (PCD) with 15 wt% Nb binder,” *Diamond and related materials,* vol. 106, p. 107867, 2020.

8 Appendix A

8.1 Relevant literature to ATOP application

Hybrid laser processing is a process of considerable interest when it comes to processing copper. This is due to its problems with absorptivities as the laser wavelength increases and approaches the IR wavelength used in the majority of current production lasers. Hybrid in this context means the use of a green (532nm) wavelength laser to initiate the melt pool and an IR (1080nm) laser to apply energy to the weld if necessary to create a deeper weld pool.

Green lasers have seen wide application to the problems of working with copper. In investigations of LPBF, the absorptivity of a copper substrate was demonstrated to start at 45% with a 515nm laser [48] this rose to 80-85% once a molten phase was achieved, as would be seen in a welding application. In an examination of hybrid welding using a blue – IR system Wu et. al. [49] found that the combination of the blue laser, which has an even higher absorptivity of around 60% than green does for copper, and the IR laser lead to a stabilisation of the energy input from the IR laser. This resulted in a calculated combined absorptive efficiency of 36% for the process compared to the 5% to be expected from a standard IR source for welding.

Similar effects were shown by Nakashiba et. al. [50] who demonstrated the difference in effect on a copper workpiece by frequency doubling a laser and showed an absorptive efficiency of around 36%. They showed the successful generation of a keyhole weld, rather than just a conductive weld, using a 1kW peak power millisecond pulsed laser. Due to the high thermal conductivity of copper, if keyhole generation is what is desired for a weld it can be challenging to supply a sufficiently high energy input rate, which a green laser is better able to provide because it absorbs a higher proportion of the input energy.

The stability of the process just mentioned is likely a result of the changing absorptivity of copper to IR wavelengths, which increases with temperature. At a threshold point of around 1350 Kelvin it increases from 8% to around 13% [51], which is an increase of around 60% in the energy absorbed. This should lead to a greater process stability as well as efficiency because a higher proportion of the IR energy will be absorbed and any effects that reduce absorbed energy are proportionally less significant

Hess et. al. [52] successfully demonstrated Green-IR hybrid welding with a green laser serving as a precursor to an IR laser. They showed a significant reduction in weld ejections, hence a higher weld quality, and an increase in absorptivity from around 6% to 11%, in line with previous figures as well as an increase in power transmitted to the workpiece from 73W to 91W. With the higher absorption of copper as it crosses its melting point the process should be more stable as any inconsistencies in the process are a lower overall percentage of the power input.

There is significant evidence of shorter wavelength hybrid laser welding being used successfully in a number of copper welding and other laser applications and the developments that are reported display sufficient progress to be optimistic about reaching the targets that ATOP has of increased quality and reduced cost from the FLASH system

8.2 Relevant literature to TOFAS application

The TOFAS case is split into 3 distinct processes, preparation, dissimilar welding and post-weld cleaning.

The problems with the welding of aluminium alloys generally start with its tenacious oxide layer. This layer has a tendency to form hydrogen porosity in the weld owing to as well as disruption of the weld pool owing to the difference in thermal and other characteristics between aluminium oxide and the base metal [53]. Therefore removing it is going to be a necessary part, along with the removal of any other contaminants. Zhou et. al. [16] demonstrated the effectiveness of nanosecond and picosecond cleaning on 5A06 aluminium substrate. The first point of interest that was demonstrated was that the nanosecond laser had significant formation of a molten phase, this resulted in an oxygen content of 5.6% when processed in air and 2.1% in argon, compared to 4.3% in air and 0.7% in argon from the picosecond. This is not surprising given that elevated temperatures will lead to a more rapid reformation of the oxide layer. Both however demonstrated a significant drop from the original oxygen mass fraction of 11.5%. The ultimate result was a reduction in the porosity of the final seam from 9.7% to a minimum of 1.6% under argon which is a significant improvement.

Laser cleaning has also been employed in filler based welding processes as would be employed in may sectors of the automotive industry by AlShaer et. al. [54] they employed a ns pulsed Nd:YAG laser to clean AA6014 alloy and achieved significantly positive results using representative fillet and flange joints. They achieved a reduction in surface roughness of the weld from 982nm to 882nm of the joints and an observable removal of multiple elemental contaminants from the surface. Most importantly they reduced the porosity from between 10-80% on the uncleaned joints to consistently below 1% in both types of joints. Given the complex interactions that already happen in dissimilar welding between steel and aluminium this demonstrates that it will be important to achieve good parameters to prepare the joint and remove as many contaminants as possible before the process. Another fact it demonstrates is that even in pure aluminium joints the use of a filler metal often used, so this is likely to be necessary for Al-Steel dissimilar joints.

For joins in automotive between steel and aluminium there is a tendency to use a brazing approach, Filliard et. al. [55] demonstrated high rates of welding of between 4-6m/min, however that speed will not be replicable in the FLASH system as it stands given the rating of their laser source and the use of a hot wire feed for the brazing filler. They were able to limit intermetallic layer thickness to below 8µm. It is however worth noting that the maximum strength that they achieved was only around 120 MPa with Al6016 and Al 4043 filler wire. This is a consistent problem with the use of aluminium alloys suitable for welding (5xxx or 6xxx) and is noted in other work such as Frank [20] who achieved maximum strengths of 160MPa with 6082 and AlSi12 filler and is caused by the limit of strength of the filler metal.

Selection of the correct filler metal is a significant component in the creation of a good quality joint. In a study of 5 separate filler metals Yu et. al. [56] found differences from 131 MPa with pure aluminium to 188 MPa with AlSi5. Brazed joint investigations from other researchers in steel and aluminium have a tensile strength range of 150-200MPa [57] [58]. However even with brazed joints there remains significant problems with corrosion in dissimilar joining as explored by Shi et. al. [59].

There are a few reasons for the preference for the filler approach, the strong galvanic corrosion potential between steel and aluminium and also the poor solubility of the two metals leading to thick IMC formation as well as the high shrinkage of aluminium metal leading to stress and shrinkage in the weld. Generally speaking, the welding potential of Aluminium and Ferrous metals is considered poor [60] with the formation of a brittle intermetallic compound which has significantly degraded mechanical performance as well as problems of stress corrosion cracking. Martinsen et. al. [61] provide a summary of many approaches to resolve this problem in the automotive sector.

Lining layers are another approach to deal with both dissimilar welding between aluminium and steel. Kang et. al. [14] investigated the joining of 6082-grade aluminium and SUS301L-DLT stainless steel by using a nickel film interlayer. The purpose of the interlayer is to try and expand the volume of the melt pool to deal with the high level of shrinkage experienced by Aluminium as it goes through its liquid and solid phase transformation. It was also found that the thickness of the intermetallic layers in the welds was decreased and there was a formation of aluminium and Iron nickel intermetallics. They claim an increase of 43% in weld tensile properties but the figures they produce for tensile strength are not in line with what might be reasonably expected and so are somewhat questionable and would need to be confirmed independently. Their welding speed also capped out at an ideal rate of roughly 5 mm/s.

Regardless of the approach there are likely to be significant problems with cracking to try and overcome in this application and that is likely to be the chief challenge for this use case.

8.3 Relevant literature to DPS application

Drilling titanium at the thicknesses required by DPS and maintaining the required tolerances and quality is likely to be a source of particular challenge. The thickness ranges from 2-6mm across the cup and tolerances of between 0.01 and 0.2mm.

Ahmed et. al. [62] used a Nd:YAG laser with a 10 μs pulse duration at a 30W average power employing a multiple pass strategy to do surface micromachining such as might be employed to make the anti rotation features of the DPS hip-cup. Ahmed et al. only took machining to a depth of around 0.5mm, though with a feature size of 3 x 5mm in X/Y. What they found was that its possible to achieve an accuracy of 9μm when machining these features via a systematic DOE approach. There will be issues in trying to achieve this over a wider range because as the machined feature approaches a greater depth it will start to run into problems with exceeding the Rayleigh length of the laser. The FLASH system has two possibilities for addressing this, the first is the Zwobbel Z-shift optics which should enable the shifting of the focal point such that this accuracy can be maintained across any depth within the optics working range. The second is the inclusion of the WJGL which can also act in a similar fashion means that it is likely to be a solvable problem.

Given the long life of any implant, differences in the effect on the substrate of laser machining compared to conventional will have to be investigated. Longer pulse laser machining generally has the unavoidable consequence of HAZ on the part. Pramanik and Basak [63] summarise a number of papers on the thermal effect of lasers on titanium parts. Certain relevant highlight papers from that review include Shanjin & Yang [64] who have several findings in their investigation of a 350W millisecond pulsed laser on 1mm thick TC1 sheet. The first finding was that the choice of assist gas is extremely important owing to the reactivity of the metal to keep the HAZ under control, with HAZ's varying from 22 to 6 microns depending on whether air or argon was used and that a decrease in mechanical properties was observed when not employing an argon assist gas. Similar results were reported by Almeida et. al. [65] who noted that use of Helium and Argon assist gas produced a more regular cut surface with Ti-64 using a 600μs pulsed laser with an average power of

5300W. Both of these pulse duration values are in a similar range to the proposed cutting laser for the FLASH system and so should be replicable.

WJGL systems have been mentioned as another method for ensuring consistency of cut quality in thicker section workpieces. This has been explored by Bektas et. al. [66] when they investigated the Synova WJGL and its performance against conventional LBM cutting in a range of materials.Directly relevant to this application is an investigation in Ti6Al4V. The advantages that they found was that Ra and Rz of the hole surfaces was significantly reduced in all tested materials, specifically with titanium Rz went down from 20.44 to 13.84. Given the thickness of the material was only 0.8mm the representative nature of Ra reported is not certain, what we can infer from that Rz is that accuracy was +/- roughly 7μm which should place it within the appropriate accuracy range desired for the fine features that DPS want to be machined. Given the nature of the WJGL this accuracy should be able to be maintained across the depth of the material. Taper showed similar improvements, with an improvement from 8.3 degrees to 1.2 degrees indicating good consistency down the feature, and the recast layer saw another decrease from 19.8μm to 8.7μm, this level of control should minimise any subsequent processing steps needed for these features. The one issue with WJGL is that of speed, the measured one pass depth in the relevant material was only 181μm so speed work may need to be done to achieve the desired features in a useful time for manufacture that could sacrifice some of that quality.

Adelmann et. al. [67] investigated the effects of WJGL on much thicker section titanium, they successfully cut up to 4.7mm of titanium which places that within the range of cutting desired for this application. They also observe extremely low kerf values but do not state specifically what they are. The most important observation from their investigation however is that the beam attenuates down the cut surface of the material. Once the cut begins the beam is no longer trapped in the water jet via internal reflection and it starts to absorb in the walls of the material. The relationship that they observe of material removal per pass is asymptotic to a certain depth based on the power. The fact that the relationship is close to linear between the laser power and the ultimate cut depth supports that assessment of why there is an upper limit of cut depth and why that limit differs in different metals that have different absorptivity. They employ a 40W laser source which is easily within the capabilities of the FLASH system and if deeper cuts are desired it may be possible to run at a higher power.

The production of small surface features is explored by Liu et. al. [68] who take a design of experiments approach to find an optimised parameter set for microgroove production. They were able to successfully produce 470 micron deep grooves to a high degree of accuracy to their predictive model having a maximum error of 6.47%. The consequence of this is that for the machine learning component of flash there is good likelihood that this process should be very compatible because it is stable and predictable. It also demonstrates the accuracy of the features created, there was a maximum error of around 8.1 microns on the accuracy of the features on the X/Y plane of the test substrate.

8.4 Relevant literature to DIA application

DIA is interested in two main applications from FLASH, the first is the initial shaping via sintering of PCD onto a WC tool shank, and subsequent shaping of that PCD to a useful cutting geometry. The other is in production of CBN grinding wheels with a more regular structure to enhance performance.

Sintering of WC and binder materials has been explored by Cavaleiro et. al. [69] who processed powder using a 50W laser from a SLS additive system, they investigated the use of a stainless steel film which had been shown to enhance the densification of WC by others [70]. WC is a material that has some issues with rapid heating or cooling which can lead to cracking and so presents some challenges in laser processing. However they were able to demonstrate a finish close to that of conventional sintering with no significant issues of elemental losses or evidence of cracking. It should be possible to repeat this for PCD however care will have to be taken to avoid the issues highlighted of cracking for WC sintering.

Pacella et. al. [71] used a μs pulsed laser of 100W power to ablate PCD to the micron scale, this would be necessary to shape the tools, particularly drill flutes and to engage in wider refinement of any sintered tool. They found an ablation depth of around 5-6μm per pulse in this material varying across the ablated spot which indicates that it should be quite possible to shape a sintered tool to an appropriate cutting geometry. One observation that they did make was that there was a variation in elemental loss across the ablated area depending on the fluence. This follows given that the binder material will have a different ablation threshold and behaviors compared to the abrasive embeds but does indicate that investigation of experimental loss will be needed to ensure the tools are remaining at an appropriate composition. Ablation has been studied at a variety of wavelengths by a variety of people including Dondieu et. al. [72] in the picosecond range and Eberle & Wegener [73] in the nanosecond and picosecond range and so should not present too much of an obstacle in the context of the FLASH system.

Fernandes-Lucio et. al. [74] investigated the production of a grooved chipbreaker on PCD tools, they employed a nanosecond laser at a pulse duration of 250ns and a power of 50w. They managed to form etched patterns of up to 290μm in depth in the PCD and chipbreakers to an accuracy of 19μm difference in the heights. This research demonstrates two things of interest to FLASH. The first is that using a ns laser which shares its capabilities with the lasers to be used in FLASH it is very possible to deliberately and accurately functionalise a PCD surface and can produce a surface which has the consistency and structures necessary for this application. The second is that they were not able to statistically alter the final surface finish using this functionalisation, this means that a thorough investigation of what form of surface structuring is employed for the tool will need to be conducted to realise those benefits.

Yin et. al. [75] explored the structuring of a PCD grinding wheel using a 250fs laser in depth and did a comparison to a standard electroplated PCD wheel in a straight comparison in grinding carbide, a challenging substrate for mechanical tools. They explored a range of depths, from 4 to 10 μm and feed rates of 10-40mm/min. What they consistently found at every stage was that the structured grinding tool had a lower force, with a drop from 25 to 17.5 N normal force at 4 micron and 40mm/min and 15 to 11.5N drop in tangential force at the same rate. This scale of drop is consistent at all feeds and depths. They also found an improvement in surface Ra from 0.12μm to 0.08μm with the same parameters and that improvement was typical. What this demonstrates is that with careful design there is a definite advantage to be found in surface texturing on grinding tools.

Those two papers have been reported on in some depth but there are significant quantities of other research in the area of structuring high performance mechanical tools by Denkena et. al. [76] who investigated turning tools constructed of BN and found an increase in tool life, and Fang & Klein [77] who demonstrated structuring of PCD and a reduction in frictional forces on the structured tools among many others. There is a good likelihood of the ability to shape, structure and form the tools to achieve the end goals of DIA.

__________ END OF DOCUMENT _________